Author response to the reviewers comment from Timothy Hill on the manuscript amt-2018-392: “Low-cost eddy covariance: a case study of evapotranspiration over agroforestry in Germany”

We thank you for your feedback, suggestions and helpful comments on the manuscript. In the current document we give a point-by-point answer on above mentioned referee report. We show first the referee comments (**RC**) and secondly the answer of the authors (**AR**). Changes made in the manuscript can be found in the track changes document attached to the current document. Figure numbers and references refer to the track-changes document, if not otherwise stated.

1. RC: *This manuscript provides an interesting approach to low cost ET measurements that have been tested at large number of sites and is a useful addition to the literature. The instrumental approaches described are shown to be effective in comparisons with the LI-7200 systems. The comparison of cumulative ET (Figure 11) is impressive – it would be informative to show cumulative ET lines (perhaps in appendix) to illustrate if the seasonal responses are comparable. Furthermore it would be worth a look in the literature to put in context the size of the differences (are they close to the disagreement between conventional systems).*

1. AR: Figure 16 shows the cumulative sum of half-hourly evapotranspiration rates for the respective campaign times of approximately four weeks duration. The data were filtered for implausible values and gaps were not filled for this analysis to reduce the inferred error caused by gap-filling. We included the cumulative ET lines for the respective campaign periods in Figure 17. The figure points out that both set-ups recover properly the temporal changes of evapotranspiration during the campaign periods, caused by the plant physiological response of the underlying ecosystem to changes in meteorological driver such as incident radiation, air temperature and the vapour pressure deficit. The difference between both set-ups at the Dornburg AF site was caused by a period of bad performance of the low-cost system. If the period was discarded from the data, the difference between EC and EC-LC at the Dornburg AF site was comparable to differences at the other sites, as shown in Figure 16. We included figures 16 and 17 as shown in the current document. Regarding the comparison of differences found for the low-cost set-up with conventional systems, we included some literature (including your publication) in Section 3.7 of the manuscript.

Changes in the manuscript:

Currently, the authors of the only known study published by Hill et al. (2017) presents a low-cost EC set-up for measurements of CO_2 and water vapour fluxes. The authors compared the low-cost EC set-up with a LI-7500 gas analyser sharing the same Campbell Scientific CSAT3 sonic anemometer. They reported a 6 % flux magnitude overestimation of the latent heat flux obtained by the low-cost EC system relative to the reference EC set-up.

Flux magnitude differences observed for our low-cost set-up are comparable to flux magnitude differences between conventional EC set-ups observed in a recently published study by Polonik et al. (2019). The authors found average differences between 4 % and 14 % between water vapour fluxes obtained by different EC set-ups consisting of three different sonic anemometers and five conventional gas analysers.

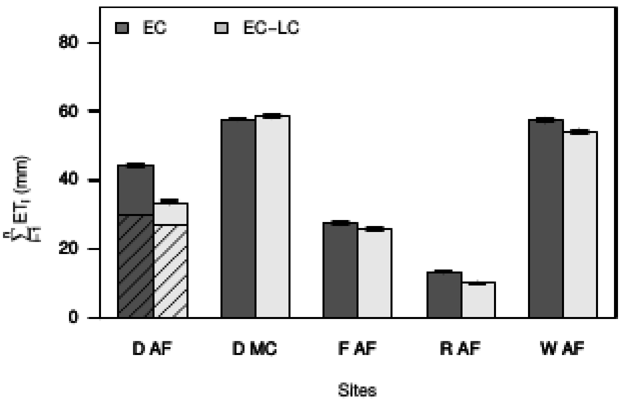

Figure 16. Cumulative evapotranspiration rates for the EC and EC-LC set-ups for Dornburg agroforestry, (D AF), Dornburg monoculture, (D MC), Forst agroforestry, (F AF)~~and~~, Wendhausen agroforestry, (W AF), and Reiffenhausen agroforestry, (R AF) over the respective campaign periods (Table A2). The error bars correspond to the summed random uncertainties~~, which were added~~. The shaded area at Dornburg agroforestry correspond to the cumulative ~~evapotranspiration rates~~sum of ET filtered for the period of poor performance of the EC-LC set-up. Incomplete records with either of EC or EC-LC missing were omitted.

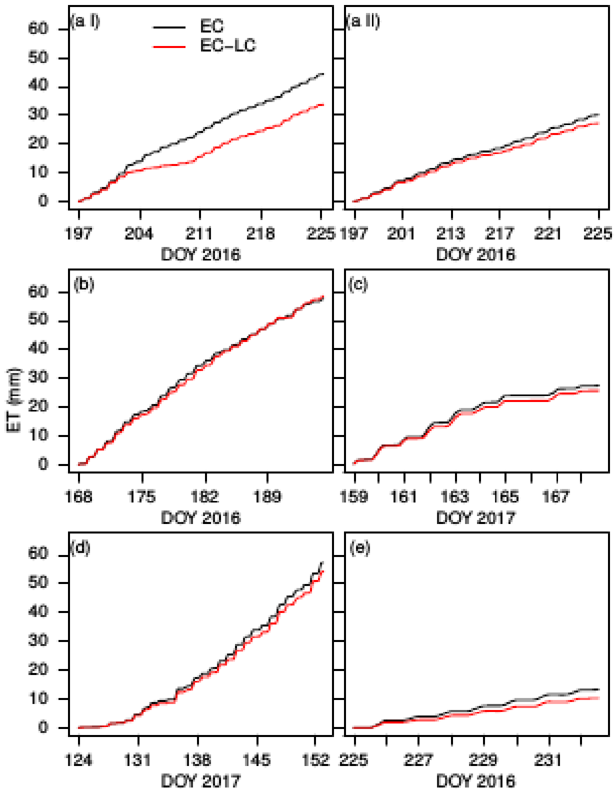

Figure 17. 30-minute cumulative evapotranspiration rates for the EC (solid black line) and EC-LC (solid red line) set-ups for Dornburg agroforestry with unfiltered data for the period of poor performance of the EC-LC set-up, (a I), Dornburg agroforestry with filtered data for the period of poor performance of the EC-LC set-up, (a II), Dornburg monoculture, (b), Forst agroforestry, (c), Wendhausen agroforestry, (d), and Reiffenhausen agroforestry, (e), over the respective campaign periods (Table A2). Incomplete records with either of EC or EC-LC missing were omitted.

3.10 Cumulative evapotranspiration rates

We observed a lower cumulative evapotranspiration for the EC-LC set-up at all agroforestry plots, ~~compared~~ relative to the conventional EC set-up (Fig. 16 and 17). In contrast, a higher cumulative ET was found for the EC-LC set-up at the monocultural agriculture plot of Dornburg. The plot of cumulative ET lines in Figure 17 (a I) indicates a discrepancy between the cumulative ET lines at the agroforestry plot of Dornburg. This is caused by a period of poor performance of the low-cost set-up. After removing this period from the data set, we still observed higher ET sums at the AF than at the MC plot, but now differences were comparable to differences observed at the other plots, as indicated by the black and red bars in Figure 16. In general, the observation of underestimated or overestimated (agroforestry vs. monocultural plots) ET rates obtained by the EC-LC ~~compared~~ set-up relative to the EC set-up ~~are~~ is in agreement with the linear regression results presented in Section 3.7.

2. RC: *My first main comment is that I would please like to see are details on: 1) the cost (since this is a low cost system, how low cost is it?); 2) power usage; 3) construction (details needed for people to replicate the build), and 4) maintenance of the low cost system. I see these details as extremely valuable for any readers to replicate this study.*

2. AR: We included more required information in the section "Instrumental set-up - Low-cost eddy-covariance (EC-LC) installation".

Changes in the manuscript:

2.2.3 Low-cost eddy-covariance (EC-LC) installation

The low-cost eddy-covariance set-up ~~comprised of~~ shared the same ultrasonic anemometer (uSONIC3-omni) as used for the conventional EC ~~method and a~~ set-up. The water vapour mole fraction was derived from the combined digital pressure, relative humidity and air temperature sensor ~~(~~BME280 ~~,~~ manufactured by *Robert Bosch GmbH*, Stuttgart, Germany ~~)~~ (hereafter named thermohygrometer, Fig. 2 depicts the low-cost set-up). The measuring principle is resistive, capacitive and based on diode voltage measurements for the air pressure, humidity and temperature sensor, respectively. The ultrasonic anemometer measured the three-dimensional wind speed and the ultrasonic temperature at a frequency of 20 Hz, whereas the thermohygrometer measured the air temperature, relative humidity and air pressure at a sampling frequency of 8 Hz. The specified response time of the thermohygrometer for relative humidity measurements is 1 s to overcome 63 % of a step change from 90 % to 0 % or 0 % to 90 % relative humidity ~~,~~ at 25 °C air temperature.

The thermohygrometer was placed 0.5 m below the centre of the sonic anemometer in a PVC housing to protect the thermohygrometer from precipitation. ~~A~~ The PVC housing consisted of an outer and an inner cylinder. The inner cylinder was perforated on the top to provide a continuous air flow of 15 lpm, generated by a ventilator (HA30101V3-0000-A99, *Sunonwealth Electric Machine Industry Co. Ltd.*, Fresnes Cedex, France). The ventilator was placed below the thermohygrometer ~~provided a continuous air flow of 15 lpm.~~ inside the inner cylinder. The volume of the inner cylinder was 98.1 cm^3.

The absolute accuracy tolerance of the ~~thermohygrometer~~ relative humidity sensor was specified as ± 3 % ~~relative humidity (Bosch Sensortec GmbH, 2016). Data~~ for 20 to 80% relative humidity at 25 °C, for the temperature sensor an absolute accuracy tolerance of ± 0.5 °C at 25 °C and ± 1 °C for a temperature range of 0 to 65 °C was specified and for the pressure sensor an absolute accuracy tolerance of ± 1 hPa (300-1100 hPa, 0-65 °C) (Bosch Sensortec GmbH, 2016).

Digital data from the thermohygrometer were recorded via the i2c protocol and stored on a RaspberryPi model B+ (*Raspberry Pi Foundation*, Cambridge, UK). The potential of the low-cost EC set-up are replicated measurements of evapotranspiration across different ecosystems. The relative cost of the low-cost set-up (featuring a sonic anemometer, a RaspberryPi and the thermohygrometer of low cost) is about 8-10 % of a conventional EC set-up.

The thermohygrometer points out with very low power consumption of approximately 3.6 μA at a sampling frequency of 1 Hz (9.4e-5 W at 8 Hz, powered with 3.3 V and if all three variables are measured simultaneously) and the RaspberryPi has a maximum power consumption of about 1.1 W if all three variables are measured at the same time. The set-up requires low maintenance. The sensors needs to be properly installed, such as they are protected against precipitation. Furthermore, a stable power supply is required. Currently, two out of ten sensors were deployed for a duration of two years.

3. RC: *The second main comment I have is that it would be very informative to see details about the actual frequency response of the low cost sensors (RH and T) and if there are environmental dependencies on these response times. It would be good to see a comparison of the sensor specification and actual response times derived from the spectral analyses. A related point is, what was the size of the frequency response correction?*

3. AR: In the following we want to address the spectral response characteristics of the BME280 thermohygrometer in two ways, first, in terms of the cut-off frequency and as the derived sensor time constant and, second, in terms of the spectral correction factor for water vapour.

Changes in the manuscript:

1. Cut-off frequency and sensor time constant

We included a new section (Section 3.4: Sensor cut-off frequency and time constant) on the sensors cut-off frequency and time constant into the manuscript and showed the dependency of the time constant on relative humidity (Figure 8).

3.4 Sensor cut-off frequency and time constant

The nominal time response of the relative humidity sensor as part of the thermohygrometer yields a theoretical sensor cut-off frequency of 0.16 Hz (6.3 s) calculated from Eq. 13.

Under field conditions we observed a mean cut-off frequency of 0.063 ± 0.02 Hz for the low-cost thermohygrometer and 0.3 ± 0.2 Hz for the LI-7200 gas analyser across five plots and all humidity classes (from 30 % to 90 % relative humidity bins). The respective mean time constant was 2.8 ± 1 s for the low-cost thermohygrometer and 0.6 ± 0.3 s for the LI-7200 gas analyser (see Fig. 8). For both sensors we found an exponential increase of the time constant with relative humidity (see Fig. 8).

Under field conditions, the cut-off frequency and the respective time constant of the thermohygrometer were inferior to the one given in the specifications. We interpret this as caused by the design of the enclosure. The thermohygrometer is placed at the end of a cylinder with the ventilator directly below, so that the flow velocity is decelerated. Subsequently, the decelerated flow velocity leads to a limited signal response. One suggestion for improvement of the frequency response would be to place the thermohygrometer inside a longer tube with a freely moving air stream. This ensures a faster air exchange inside the measurement cell of the thermohygrometer and hence a faster response time.

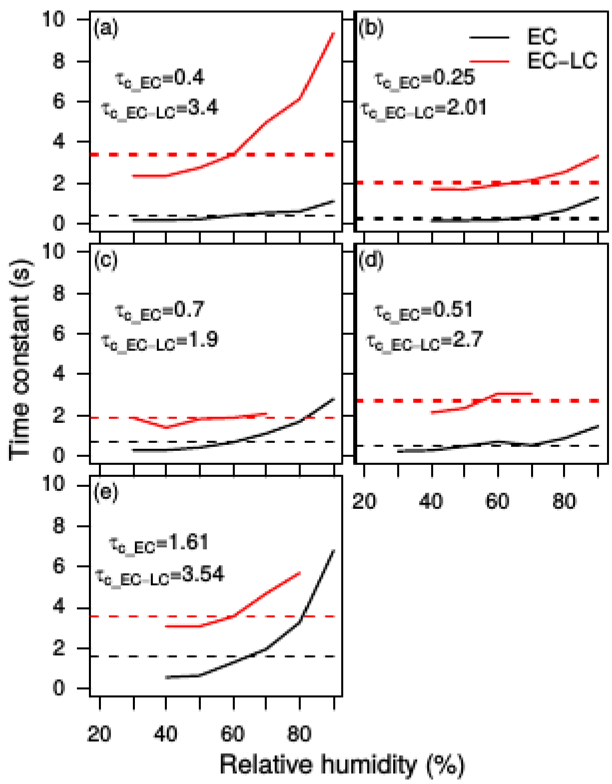

Figure 8. Time constant against relative humidity for the LI-7200 (black solid lines) and the thermohygrometer (red solid lines). Dashed lines with the same colour coding as for data shown and values written, correspond to the mean time constant for the respective sensors across all relative humidity classes. Sites correspond to Dornburg agroforestry, (a), Dornburg monoculture, (b), Forst agroforestry, (c), Reiffenhausen agroforestry, (d), and Wendhausen agroforestry, (e).

2. Spectral correction factor for water vapour

Site	Spectral correction factor (-)		Spectral correction factor flux magnitude change (%)	
Method	**EC**	**EC-LC**	**EC**	**EC-LC**
Dornburg AF	1.11	1.76	6.9	40.82
Dornburg MC	1.21	3.01	14.3	60.9
Forst AF	1.1	1.99	9.9	47.7
Reiffenhausen AF	1.11	1.31	9.4	42.3
Wendhausen AF	1.16	1.74	5.9	21.83
Mean+-sd	**1.14** ± 0.05	**1.962** ± 0.64	**9.28** ± 3.3	**42.7** ± 14.1

Table 1: Median spectral correction factor and the impact of the spectral correction factor on the flux magnitude change.

We found a higher frequency correction factor for water fluxes (combines the correction for high and low-frequency losses) obtained by the EC-LC set-up than for the EC set-up with a median flux increase of 97.4% and 14.6% (see Table 1 and Figure 6 a), respectively.

The effect of the spectral corrections on a flux magnitude increase was most pronounced for the low-cost set-up than for the conventional EC set-up with an overall flux magnitude increase of 42.7 ± 14.1 % and 9.28 ± 3.3 % for the EC-LC and the EC set-up, respectively (see Figure 3 and Table 1 of the current document).

We found the highest median spectral correction factor (3.01) and the highest flux magnitude increase (60.9%) caused by the high-frequency correction for the low-cost set-up of the monocultural agriculture plot of Dornburg. We interpret the higher spectral correction factor as caused by different measurement heights, with a measurement height of 3.5 m at the monocultural agriculture plot of Dornburg and a measurement height of 10 m at the agroforestry plot of Dornburg. At the lower tower high frequency eddies are more likely than at the taller tower. As the nominal time response (1 s) given in the specifications and the estimated time response are quite low, the flux loss is high and needs to be corrected for.

We included information on the spectral correction factor into Section 3.3 (“Effect of spectral- and WPL corrections on evapotranspiration rates from low-cost eddy covariance”) and Figure 7 into the manuscript.

The overall impact of spectral corrections on a change of the turbulent latent heat fluxes was stronger for the EC-LC set-up compared to the EC set-up. Here, we quantify the overall impact of spectral corrections on latent heat fluxes in terms of the spectral correction factor (SCF) calculated for each 30-minute period. The 30-minute SCF was multiplied with the respective uncorrected flux. A SCF larger than one indicates a flux magnitude increase, whereas a SCF lower than one indicates a flux magnitude decrease. Box-whisker plots of 30-minute SCFs for each site and each set-up are shown in Figure 7 (a). We found a mean SCF of 1.96 ± 0.64

for the EC-LC set-up and 1.14 ± 0.05 for the EC set-up across all sites, indicating a mean flux magnitude increase of 96 % for the EC-LC set-up and a mean flux magnitude increase of 14 % for the EC set-up. The mean SCF presented here integrates both night and day time periods. Thus, a high SCF during night time with commonly low latent heat fluxes leads to a smaller change of the flux magnitude than during day time, when fluxes are commonly high. Therefore, we also present the sum of 30-minute ET rates corrected for spectral losses and the sum of the total ET attributed to the spectral corrections in Figure 7 (b). The part of the total corrected ET attributed to the spectral corrections was higher for the EC-LC set-up compared to the EC-set-up and amounted on average to 42.7 ± 14.1 % of total ET for the EC-LC set-up and 9.3 ± 3.3 % of total ET for the EC set-up.

Across sites, we found the highest median spectral correction factor of 3.01 and the highest part of the total corrected ET attributed to the spectral corrections of 60.9 % for the EC-LC set-up at the monocultural agriculture plot of Dornburg. We interpret this as a measurement height dependency of the spectral corrections. The measurement height at the agroforestry plots was 10 m and at the monocultural agriculture plots the measurement height was 3.5 m. We assume that high-frequency eddies are more likely close to the surface. Therefore, a detected turbulent signal at the lower measurement height would be shifted towards high frequencies compared to the detected turbulent signal at the higher measurement height (Aubinet et al., 2012). If a sensor is not capable of detecting the turbulent signal in the high frequency range of the spectrum, the signal is attenuated and needs to be corrected.

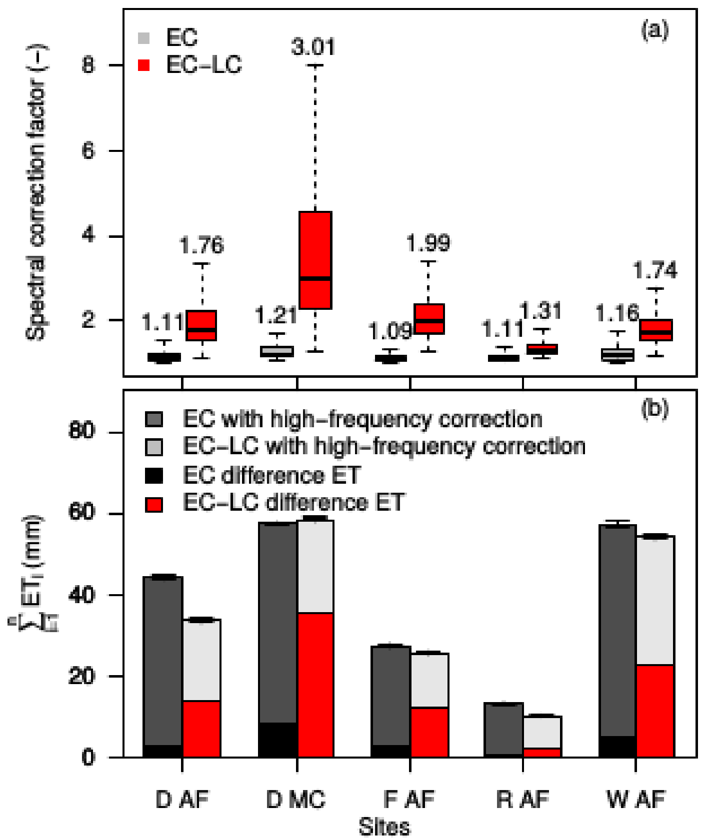

Figure 7. a) Box-whisker plot of spectral correction factors for the EC (grey) and the EC-LC (red) set-up for all sites. Values above the bars correspond to the median spectral correction factor, and, b) cumulative evapotranspiration rates for the EC and EC-LC set-ups for all sites, e.g Dornburg agroforestry, (D AF), Dornburg monoculture, (D MC), Forst agroforestry, (F AF), Wendhausen agroforestry, (W AF), and Reiffenhausen agroforestry, (R AF), over the respective campaign periods (Table A2). The error bars in Figure (b) correspond to the summed random uncertainties. The black and red bars correspond to that part of the total ET attributed to the high-frequency correction for the EC and EC-LC set-up, respectively. Incomplete records with either of EC or EC-LC missing were omitted.

4. RC: *My third main query is what did the energy balance closures look like? ALthough an incomplete assessment of the ET, it would be informative to know the closure for the systems and sites.*

4. AR: We estimated the energy balance closure (EBC) of both systems at all sites. For the sites shown in the current manuscript we found EBCs similar to agricultural fields with a maximum of 88% and a minimum of 76% for the conventional EC set-up. The EBC of the low-cost set-up was lower relative to the conventional EC set-up at the agroforestry plots, according to an observed underestimation of the latent heat fluxes at those sites. Whereas, at the monoculture sites the EBC was higher for the low-cost set-up compared to the conventional EC set-up according to overestimated latent heat fluxes relative to conventional EC. Further analysis on the EBC is part of a separate study, currently in internal review.

5. RC: *Abstract: - A (pedantic) comment on the assumption that Eddy Covariance is appropriate for homogeneous land surfaces: Whilst arguably true (depending on the errors associate with EC) the assumption of homogeneity first needs to be tested using a suitable experimental design. See Hurlbert 1984 (Pseudoreplication and the Design of Ecological Field Experiments). Otherwise our implicit assumption is that the (non-flux) data we have about the full extent of the terrain (which might be limited to little more than a visual/reflectance based observations) is sufficient to predict the fluxes (or at least the variability - or lack of - in fluxes) – and if this is the case why use EC?*

5. AR: The homogeneity of the underlying surface is an assumption of the EC method. Sure, it is not possible to predict a flux from a visual based observation, but we can assess the homogeneity of the landscape/ecosystem purely visual. This includes the assumption that if the ecosystem seems homogeneous without major disturbances, the measured flux is also homogeneous at each point of the ecosystem. We therefore assume that the plant physiological response to biophysical drivers is the same for the ecosystem of interest.

Related to this discussion, the manuscript focus on an instrument comparison. We assume that the measured flux originating from the same ecosystem is the same for both set-ups (installed on the same tower) and therefore the impact of the ecosystem heterogeneity on fluxes is also the same.

Changes in the manuscript:

Abstract. ~~Eddy covariance has evolved as the method of choice for measurements of the ecosystem-atmosphere exchange of water vapour, sensible heat and trace gases. Under ideal conditions, eddy covariance provides direct and precise flux observations, commonly approximated from single point eddy covariance measurements. While eddy covariance is appropriate over uniform terrain of infinite extent, heterogeneous land surfaces compromise the representativity of single-point measurements as a predictor for ecosystem-wide fluxes and violate assumptions of the eddy covariance method. Therefore heterogeneous~~ Heterogeneous land surfaces require multiple measurement units for spatially adequate sampling and representative fluxes. The complexity and cost of traditional eddy covariance ~~instruments~~ set-ups typically limits the feasible number of sampling units. Therefore, new low-cost eddy covariance systems ~~are required~~ provide ideal opportunities for spatially replicated sampling~~, not only to increase the representativity of turbulent fluxes at a single site, but also for experiments where replication is required to e.g. compare different ecosystems~~.

The aim of this study was to test the performance of a compact low-cost pressure, temperature and relative humidity sensor for the application of evapotranspiration measurements by eddy covariance over agroforestry and conventional agriculture in Germany. We performed continuous low-cost eddy covariance measurements over agroforestry and conventional agriculture for reference, at five sites across Northern Germany over a period of two years from 2016 to 2017. We conducted side-by-side measurements using a roving enclosed-path eddy covariance set-up to assess the performance of the low-cost eddy covariance set-up.

Evapotranspiration measured with low-cost eddy covariance compared well with fluxes from conventional eddy covariance. ~~Diel cycles of evapotranspiration were well represented at a 30-min resolution. The differences between low-cost and conventional eddy covariance at 30-min resolution were small relative to the diel amplitude of the fluxes.~~ The slopes of linear regressions for evapotranspiration comparing low-cost and conventional eddy covariance set-ups ranged from 0.86 to 1.08 for five out of ten sites, indicating a 14% flux underestimation and a 8% flux overestimation relative to the conventional EC set-up, respectively. Corresponding coefficients of determination, R^2~~values~~, ranged from 0.71 to 0.94 across sites. ~~This indicates that a high proportion of the flux variability of the conventional eddy covariance set-up is reproduced by the low-cost eddy covariance set-up.~~ The root mean square error for differences between latent heat fluxes obtained by both set-ups were small compared to the overall flux magnitude, with a mean and standard deviation of 34.23 ± 3.2 W m^{-2}, respectively, across sites.

The spectral response characteristics of the low-cost eddy covariance set-up were inferior to the eddy covariance set-up in the inertial sub-range of the turbulent spectrum. The water vapour flux cospectrum of the low-cost eddy covariance set-up underestimated the theoretical slope of -4/3 stronger than the conventional eddy covariance set-up. This underestimation ~~is~~ was mainly caused by the limited response time of the low-cost thermohygrometer ~~of one second, which prevents eddies of a frequency higher than two times the response time to be adequately sampled by the thermohygrometer~~longer than one second.

We conclude that low-cost eddy covariance sensors are an alternative to conventional eddy covariance sensors when~~spatial~~, first, replicates are required ~~or when the scientific questions require a larger number of measurement units. An appropriately chosen high-frequency correction method is essential for the slow-response sensor. The new low-cost eddy covariance set-up is a viable alternative, particularly when~~and, second, the spatial variability of fluxes of the ecosystems of interest is larger than above reported set-up specific differences in fluxes.

6. RC: *-Line 8: Given the general lack of energy balance closure for the EC method, I don't think the 'true' ET flux is known. Therefore, 'underestimation' and 'overestimation' are more accurately termed 'underestimation relative to the conventional system'.*

6. AR: It was not entirely clear which line you refer to. Nevertheless, we interpreted your comment as a general one and checked the formulations throughout the whole document and changed them accordingly.

7. RC: *Page 3: Can you describe the site fetch? What are the heights of the trees and the crops? Reiffenhausen is a small site 18,700 m2 (~1.9 ha), what is beyond the extent of this site (and likely in your flux footprint)?*

7. AR: We included a purely descriptive explanation on the site fetch in Section "Site description" for the respective sites, because an extensive discussion of the flux footprint is not the scope of the current manuscript. A description and visual presentation of the flux footprint will rather be part of a manuscript currently in internal review.
Mean tree heights were included in "Table A1. Site locations, agroforestry geometry and stand characteristics" for the respective years the campaigns took place. Tree heights include the standard deviation and the number of trees included in the calculation.
Nevertheless, we think that the flux footprint information for the current manuscript is only of minor importance because it is mend to be a technical paper. Additionally, we argue that the two set-ups should effectively sample the same air and therefore the flux footprint should be the same for both set-ups. But we are aware that a comparison of different land use systems regarding the exchange of trace gasses between the ecosystem and the atmosphere require a proper evaluation of the flux footprint.

Changes in the manuscript:

1. flux footprint

We performed a flux footprint climatology analyses with the Flux Footprint Prediction online tool (http://footprint.kljun.net/, Kljun et al. (2015)). The flux footprint climatology is valid for the respective campaign and only for daytime data according to a global radiation $R_G > 20\,\mathrm{W\,m^{-2}}$. We found a 90% flux magnitude contribution of the agroforestry plot of Forst and the monoculture plot of Dornburg and a 80% flux magnitude contribution of the agroforestry plots of Dornburg and Wendhausen. The smallest agroforestry system of Reiffenhausen contributed the least to the measured turbulent flux with 60%. Outside the agroforestry plot, fluxes were affected by nearby crop fields and forests in about 400 m distance to the flux tower in northerly direction and about 200 m distance in southerly direction, respectively.

2. tree height

Table A1. Site locations~~and~~, agroforestry geometry and stand characteristics.

Site	Coordinates	No. of treealleys	System size [m^2]	Relative tree cover	Tree height [m]
Reiffenhausen	51° 24′N 9°59′E	3	18700	72%	4.73±0.32 (n=69, BHD≥1 cm)
Mariensee	52° 34′N 9°28′E	3	69260	6%	4.01 ±0.33 (n=96)
Wendhausen	52°20′N 10°38′E	6	179738	11.52%	6.21 ±0.4 (n=114)
Forst	51°47′N 14°38′E	7	391300	12%	6.5±1.8 (n=161)
Dornburg	51°47′N 11°39′E	7	508723	8%	6.4±0.64 (n=160)

8. RC: *Discussion: - I am reluctant to recommend citing my own paper, but as it is one of the only other studies to calculate ET from a low cost RH sensor, I think comparisons with the LE fluxes/approach from Hill GCB 2017 (and any others) should be made somewhere in the discussion.*

8. AR: Indeed, we apologize this and considered your study in the discussion of differences between the two different set-ups along with other studies not particularly focussing on low-cost sensors, but on the comparison of different conventional eddy covariance set-ups. We included information to Section 3.7 of the manuscript.

Changes in the manuscript:

Currently, the authors of the only known study published by Hill et al. (2017) presents a low-cost EC set-up for measurements of CO_2 and water vapour fluxes. The authors compared the low-cost EC set-up with a LI-7500 gas analyser sharing the same Campbell Scientific CSAT3 sonic anemometer. They reported a 6 % flux magnitude overestimation of the latent heat flux obtained by the low-cost EC system relative to the reference EC set-up.

Flux magnitude differences observed for our low-cost set-up are comparable to flux magnitude differences between conventional EC set-ups observed in a recently published study by Polonik et al. (2019). The authors found average differences between 4 % and 14 % between water vapour fluxes obtained by different EC set-ups consisting of three different sonic anemometers and five conventional gas analysers.

9. RC: *-Page 6 It would be useful to know the indicative cost and power usage for both systems. What is the volume of the thermohygrometer housing? What is the form of the housing? What response time (and measurement principle) did the temperature sensor of the BME280 use?*

9. AR: We included more information on the set-ups design in the revised manuscript and gave more information in AR 2 of the current document.
The response time of neither the temperature sensor nor the pressure sensor was explicitly stated in the sensor specifications. See more information on the response time in the author response 3 of the current document. The measurement principle of the temperature sensor is based on diode voltage measurements (personal communications with the manufacturer; according to the manufacturer specific details are confidential). We included more information on the measurement principle in the manuscript, please see AR 2.

10. RC: *- Page 6: it is not entirely clear to me if the systems shared the same sonic, and if not, what was the spatial separation of the comparison system?*

10. AR: Yes, the two set-ups shared the same sonic anemometer and we clarified this in the manuscript. Please see AR 2.

11. RC: *-Page 7: I am interested in how much data was filtered through QC and how you filtered data for the LC system?*

11. AR: The raw data, such as the air temperature, the relative humidity, air pressure, the 3D wind components and the sonic temperature, were filtered for upper and lower limits. The overall amount of data discarded by upper and lower limits was not significant.

Latent heat fluxes were filtered for implausible values with lower and upper limits of -50 and 500 W m^{-2}, respectively. Furthermore, all data corresponding to a quality flag of 2 were discarded following the two-stage quality procedure presented in Mauder and Foken (2011a). We further discarded latent heat fluxes according to the 97.5% percentile of the H_2O variance and we applied spike removal methods described in Vickers and Mahrt (1997). The amount of data discarded through QC for the respective campaign periods was fairly similar for both set-ups at the sites and is shown in Table 1 of the current document. We included information on the amount of data discarded to the manuscript (Section 2.2.3 Low-cost eddy-covariance (EC-LC) installation)

Site	**EC**	**EC-LC**
D AF	8.7%	13.9%
D MC	6.6%	6.8%
F AF	7.1%	6.5%
R AF	11.1%	10.3%
W AF	14.4%	14.6%

Table 1: Amount of data discarded through QC for both set-ups and all sites, e.g. Dornburg AF, “D AF”, Dornburg MC, “D MC”, Forst AF, “F AF”, Reiffenhausen AF, “R AF” and Wendhausen AF, “W AF”.

Changes in the manuscript:

a flag of 2, following the two-stage quality control procedure of Mauder and Foken (2011b). Latent heat fluxes below -50 $W\,m^{-2}$ and above 500 $W\,m^{-2}$ were discarded. We further discarded latent heat fluxes according to the 97.5% percentile of the H_2O variance and spikes were removed after Vickers and Mahrt (1997). Through quality check 9.6±3.2% and 10.4±3.8% of half-hourly latent heat fluxes were discarded for the EC and EC-LC set-up, respectively, as a mean over all five plots. Low-frequency and high-frequency losses were corrected by the procedure of Moncrieff et al. (2004) and Ibrom et al. (2007), respectively. Random uncertainties of ~~the latent heat~~ fluxes were calculated after Mann and Lenschow (1994).

12. RC: *-Page 8: It would be useful to know the time response of the temperature sensor. Figure B1 does not give a good insight into this response as it convolves: sensor response; sensor noise; housing attenuation and variability of scalar (i.e. RH or T). A look at the spectra/cospectra of the sensors (and a modelled attenuation of the sonic-T would give a much clearer idea (and quantification) of the total combined attenuation of the sensor and housing.*

12. AR: The time response of the temperature sensor was not explicitly stated in the sensor specifications. We think that information on the response time of the derived water vapour mole fraction is of major interest compared to the specific response times of each sensor, e.g. temperature, relative humidity and air pressure. Indeed, Figure B1 is not ideal to present the sensor response, we therefore removed figure B1 and estimated the sensor time constant of the temperature sensor of the BME280 in a lab experiment. The time constant of the temperature sensor was 23.3 ± 0.9 s as a mean over 4 replications. The temperature measurements are highly attenuated and can therefore be used for the calculation of the water vapour mole fraction, because now fluctuations originate from the temperature sensor.

The estimation of the time constant of the relative humidity sensor of the thermohygrometer is more complex. We expect that the specifications given by the manufacturer are correct and we rather estimated a time constant for the whole complex from water vapour spectra as stated in AR 3 of the current document.

13. RC: *-page 9: provide details here, or later on about the timelag. Are you sure this is due to the vertical separation? (if so it should be dependent on W). Alternatively it could be due to the sensor response/processing time and therefore it reasonable to expect it may include a T/RH dependency.*

13. AR: Indeed, the time lag of the low-cost system has different overlapping causes, which include the vertical sensor separation, the mentioned limited response time and the processing time, as well as a dependency on environmental factors, such as relative humidity. We are not able to separate the causes of the time lag and we decided to shorten the sentence mentioned. We will give further information about the time lag of both set-ups later.

14. RC: *-page 15: Fig6 It is interesting to see that the LI-7200 is highly attenuated and more sensitive to RH than the LC system. Indeed attenuation of the LI-7200 in panel c (and even more so in d) is significant and indicates a very poor frequency response for this system. Any thoughts on why? Did you run with filters and did they clog frequently?*

14. AR: Indeed, the frequency response is fairly poor in particular at those plots mentioned. Yes, we used filter for the EC set-up (2 µm), but exchanged those before installing the system in the field, approximately after four weeks.

One reason for the poor frequency response might be a thicker inner intake tube diameter in 2017 (inner diameter of 8.3 mm) relative to 2016 (inner diameter of 5.3 mm) as also discussed in Section 3.4.1. We kept the flow rate of 15 slpm equal in both years. The thinner tube had a Reynolds number of 3950.6 (towards turbulent flow) and the thicker tube had a Reynolds number of 2551.71 (towards laminar flow).

15. RC: *Fig 6, can you please clarify (as I assume that the RH is specific for the LI-7200 and the LC sensor (with its higher temperatures and presumably lower RH). Either way the comparison is complicated: if ambient RH is used, then the sensors are effectively seeing different RH, alternatively if sensor RH is used, then the spectra contain different data (i.e. wind speed/stability might differ). Neither point are likely to be particularly significant to the overall interpretation, but should be clarified.*

15. AR: Along with the raw data of high frequency, we provided 10 second biomet data, such as air temperature, relative humidity, global radiation and air pressure to the eddy covariance software EddyPro. If biomet data were available EddyPro use those for different flux corrections. Thus, in Fig. 6 (now Figure 8) the relative humidity classes are derived from ambient relative humidity. Sure, we agree that in this case the comparison of the two different instrumental set-ups is complicated. Nevertheless, the main purpose of this Figure was to show the spectral response characteristics in dependence on different relative humidities separately for each set-up. It was not mend to be a comparison of both set-ups at one particular relative humidity class, because the comparability is not given, as you stated. We clarified this in the manuscript.

Changes in the manuscript:

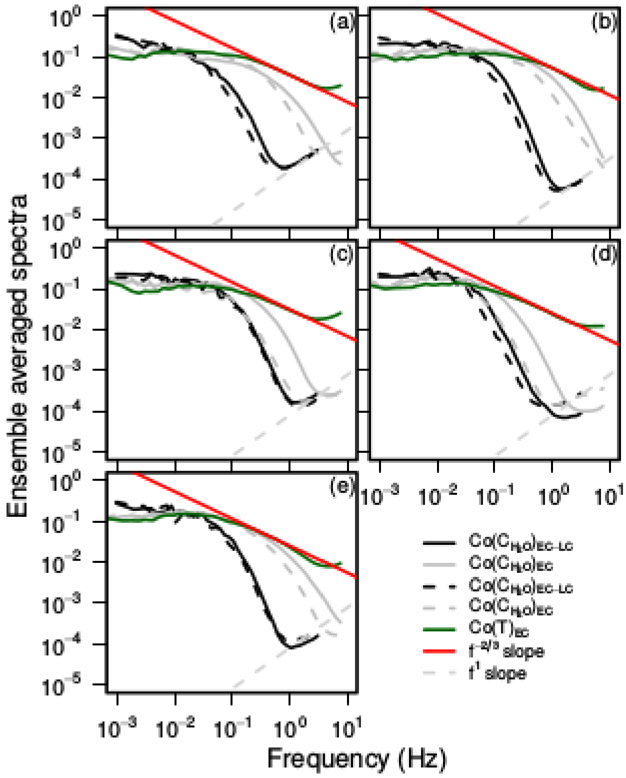

Figure 8. Ensemble averaged normalised water vapour and temperature spectra for relative humidity thresholds of 60 % (solid lines) and 80 % (dashed lines) versus the natural frequency. Spectra of the EC set-up (grey) and the EC-LC set-up (black) are shown. Subfigures correspond to plots: Dornburg agroforestry, (a), Dornburg monoculture, (b), Forst agroforestry, (c), Wendhausen agroforestry, (d), and Reiffenhausen agroforestry, (e). Spectra were filtered for low quality data, corresponding to a flag of 2 following the procedure of Mauder and Foken (2011a) and according to spike removal methods described in Vickers and Mahrt (1997). Relative humidity classes correspond to ambient relative humidity measurements from biomet readings.

16. RC: *Fig 6/7: please include the criteria for data shown, what correlation strength/LE/stability classes are included?*

16. AR: We included information on the filter criteria in the figure captions of Figures 6 (now Figure 8) and 7 (now Figure 9), respectively.

Changes in the manuscript:

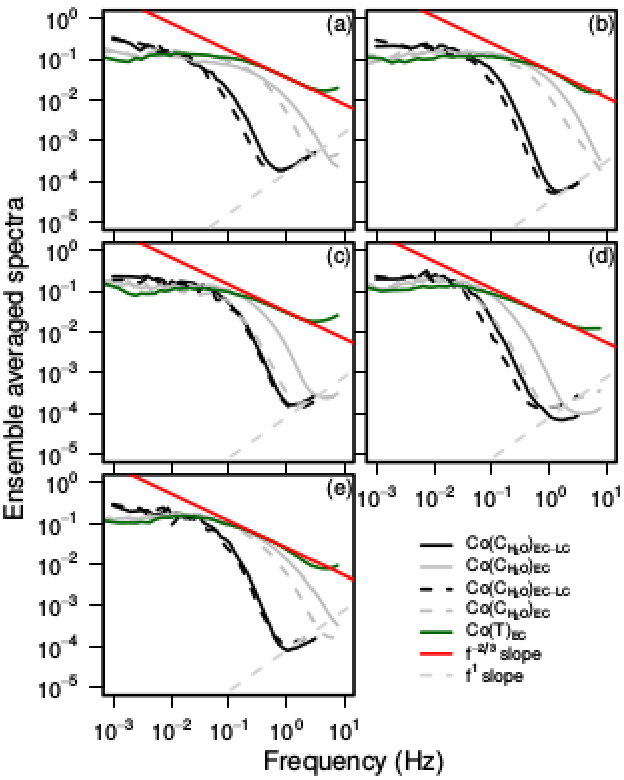

Figure 8. Ensemble averaged normalised water vapour and temperature spectra for relative humidity thresholds of 60 % (solid lines) and 80 % (dashed lines) versus the natural frequency. Spectra of the EC set-up (grey) and the EC-LC set-up (black) are shown. Subfigures correspond to plots: Dornburg agroforestry, (a), Dornburg monoculture, (b), Forst agroforestry, (c), Wendhausen agroforestry, (d), and Reiffenhausen agroforestry, (e). Spectra were filtered for low quality data, corresponding to a flag of 2 following the procedure of Mauder and Foken (2011a) and according to spike removal methods described in Vickers and Mahrt (1997). Relative humidity classes correspond to ambient relative humidity measurements from biomet readings.

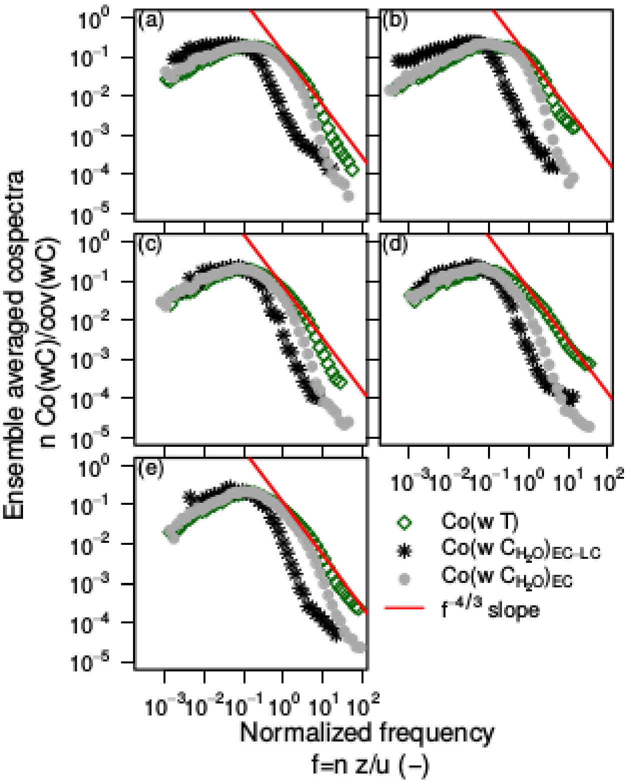

Figure 9. Ensemble averaged ~~evapotranspiration~~ cospectra of the water vapour flux for the EC- and the EC-LC ~~set-up~~ set-ups (grey and black dots, resp.) and the ~~temperature~~ cospectrum of the sensible heat flux (green dots) versus the normalized frequency over the entire campaign period for Dornburg agroforestry, (a), Dornburg monoculture, (b), Forst agroforestry, (c), Wendhausen agroforestry, (d), and Reiffenhausen agroforestry, (e). Cospectra shown correspond to an unstable stratified atmosphere according to a Monin-Obukhov length between -650<L<0. Cospectra were filtered for low quality data, corresponding to a flag of 2 following the procedure of Mauder and Foken (2011a) and according to spike removal methods described in Vickers and Mahrt (1997).

17. RC: *-Page 17: The linear regressions are very important and it would be very useful to see the scatter plots associated with these to see if they are well behaved.*

17. AR: The linear regressions between latent heat fluxes obtained by the low-cost EC set-up and the conventional EC set-up were included in Figure 11**.** We showed the scatter plots for all sites and both high-frequency spectral correction methods, e.g. Ibrom et. al. (2007) and Moncrieff et al. (1997), applied to latent heat fluxes obtained by the low-cost EC set-up. We included the linear regression equation, the coefficient of determination and the number of points used for the analysis.

Changes in the manuscript:

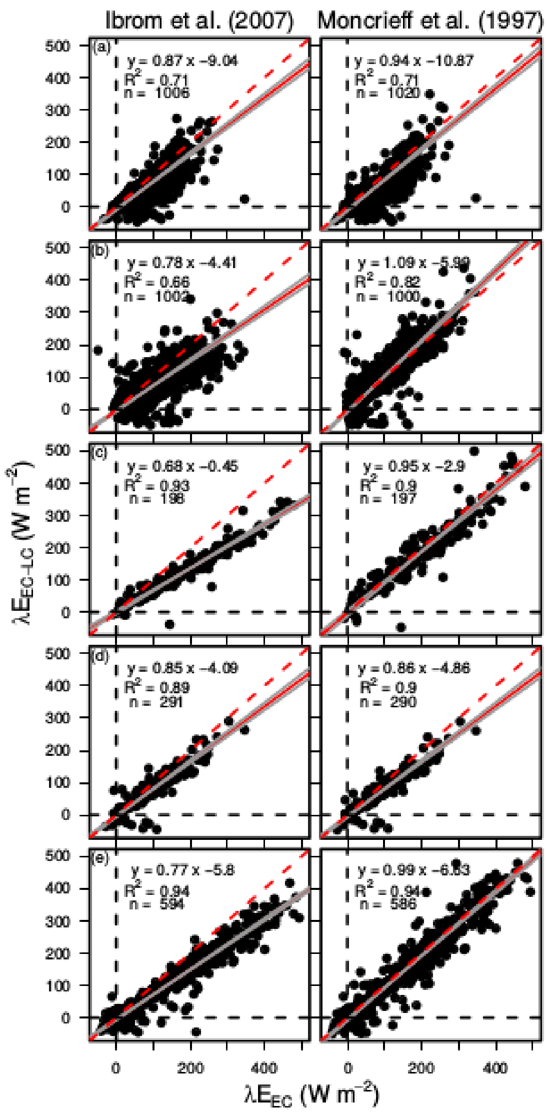

Figure 11. Scatter plots of latent heat fluxes obtained by the low-cost EC set-up versus latent heat fluxes obtained by the conventional EC set-up for Dornburg agroforestry, (a), Dornburg monoculture, (b), Forst agroforestry, (c), Reiffenhausen agroforestry, (d), and Wendhausen agroforestry, (e). For this analysis, latent heat fluxes obtained by the conventional EC set-up were corrected for high-frequency losses by the high-frequency correction method of Ibrom et al. (2007), whereas the latent heat fluxes obtained by the low-cost EC set-up were corrected by, first, the high-frequency correction method of Ibrom et al. (2007) (left site) and, second, the high-frequency correction method of Moncrieff et al. (1997) (right hand site).

18. RC: *-page 21: figure 12. It is not clear how the 2016 annual ET fluxes were arrived at given the campaign basis of the measurements. Table A3 implies some sites were not measured in 2016.*

18. AR: The data shown in this figure are independent of the campaigns. We conducted continuous measurements of evapotranspiration throughout the year 2016 at the other sites as well, independently if campaigns took place or not. The data shown here are quality checked for implausible values and are not gap-filled. We clarified this also in the manuscript.

Changes in the manuscript:

3.11 Annual cumulative ET rates for the agroforestry and the monocultural plot

We wanted to understand how evapotranspiration of agroforestry and monoculture differed. We deployed the EC-LC set-up as a convenient means to obtain continuous long-term evapotranspiration estimates at 30-minute resolution. Here, we present annual cumulative sums of 30-minute evapotranspiration rates for 2016 from all sites, independently of the measuring campaigns.

At the Dornburg site, annual cumulative evapotranspiration rates were higher at the monocultural agriculture plot compared to the agroforestry plot (Fig. 17), which might be caused by the wind-exposed location of the monocultural agriculture plot. The higher wind speed at the monocultural agriculture plot increases the boundary layer conductance and therefore both soil evaporation and plant transpiration increase.

At the remaining four out of five sites the annual cumulative evapotranspiration rates were higher at the agroforestry plots than at the monocultural agriculture plots (Forst, Wendhausen, Mariensee and Reiffenhausen, Fig. 17). We interpret higher evapotranspiration rates at the agroforestry than at the monocultural plots as an effect of the increased biomass at the agroforestry plot, originating both from the trees and the crops grown between the tree strips. Despite the presence of a leeward side with reduced evapotranspiration caused by the wind reduction and the increased shade, both crops and trees are affected by wind on the windward site. More turbulent conditions are present at the agroforestry plots as caused by the presence of the tree strips, which is indicated by a higher mean roughness length at the agroforestry plots compared to the conventional agriculture plots as shown in Fig. A1 for all sites.

Author response to the reviewers comment from Anonymous Referee #3 on the manuscript amt-2018-392: "Low-cost eddy covariance: a case study of evapotranspiration over agroforestry in Germany"

We thank you for your feedback, suggestions and helpful comments on the manuscript. In the current document we give a point-by-point answer on above mentioned referee report. We show first the referee comments (**RC**) and secondly the answer of the authors (**AR**). Changes made in the manuscript can be found in the track changes document attached to the current document. Figure numbers and references refer to the track-changes document.

1. RC: *General comments*

This manuscript presents a test of a low-cost hygrometer manufactured by Bosch GmbH being used for eddy-covariance measurements. The sonic anemometer is the same as for regular eddy-covariance system being deployed. Another difference between the low-cost system and the regular system is the data acquisition, which is realized by a Raspberry Pi instead of a Campbell CR6 data logger. The regular EC system has a Licor LI7200 for measuring water vapor and CO2 fluctuations. I doubt that the data acquisition causes significant differences in the collected data since both systems are recording digitally. So, the main question of this study is, whether the precision and the spectral response characteristics of the Bosch hygrometer are sufficient for eddy covariance applications. The results of evapotranspiration show a good agreement, if adequate spectral corrections are applied, which leads the authors to the main conclusion that this low-cost system is an alternative when a larger number of measurement units is required for a certain application. I generally agree with this assessment; however, I suggest that a more extensive evaluation of the spectral response characteristics of the Bosch sensor based on the collected field data should be presented, e.g. the system's cut-off frequency based on in-situ assessment method of Ibrom et al. (2007) and the transfer function of the Moncrieff et al. method. This would perhaps also better explain why the one method gave different results than the other.

1. AR: We included more information on the spectral response characteristics of the thermohygrometer. In detail, we derived the cut-off frequency and the sensor time constant from water vapour mole fraction spectra as a function of relative humidity. And we included information on the spectral correction factor for both the low-cost and conventional EC system. See the author response 5 of the current document for more information.

In a lab experiment we estimated the sensor time constant of the temperature sensor of the BME280. The time constant of the temperature sensor was 23.3 ± 0.9 s as a mean over 4 replications. Testing for the time constant of the relative humidity sensor requires more effort, especially proper ambient conditions are needed. We know that the response time of 1 second is the fastest we can achieve. Under field conditions the sensors response time was slower than given in the specifications. We can improve the response time by modifying the enclosure design, so that the sensor is placed in a freely moving air stream.

Thank you for your comment and suggestion on differences found between the two different high-frequency spectral corrections. One explanation of differences found for the two different high-frequency spectral corrections is the low amount of data. The in-situ assessment method of Ibrom et al. (2007) requires at least one month of data to successfully estimate the transfer functions cut-off frequency. For shorter time periods the cut-off frequency might not be appropriate. Therefore, the corrections might be performed in a wrong frequency range. In contrast, for the high-frequency correction after Moncrieff et al. (1997) a transfer function is estimated for each 30-min period and is therefore independent of the amount of data.

We included Figure 12 into the manuscript showing the combined high-frequency correction transfer function after Moncrieff et al. (1997) (sonic and thermohygrometer dynamic frequency response, sonic path averaging, attenuations inside the intake tube of the thermohygrometer for laminar flow, vertical and horizontal separation between sonic anemometer and thermohygrometer) and the infinite impulse response filter, approximated by the Lorentzian and presented in Ibrom et al. 2007. The frequency range covered by the transfer function after Ibrom et al. (2007) includes also low frequencies, whereas the transfer function after Moncrieff et al. (1997) is shifted towards high frequencies. So, low-frequency contributions are conserved.

Changes in the manuscript:

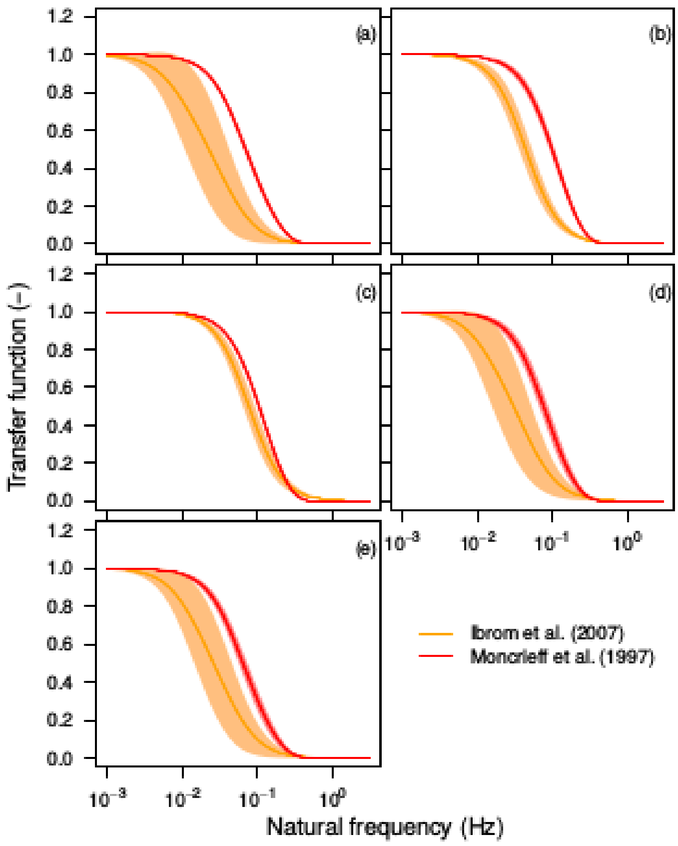

Figure 12. Mean and standard deviation of the spectral correction transfer functions vs. the natural frequency for the high-frequency spectral correction methods of Ibrom et al. (2007) and Moncrieff et al. (1997), respectively, for sites, e.g. Dornburg agroforestry, (a), Dornburg monoculture, (b), Forst agroforestry, (c), Reiffenhausen agroforestry, (d), and Wendhausen agroforestry, (e). The transfer function after Ibrom et al. (2007) represent the mean over all infinite impulse response (IIR) filter, approximated by the Lorentzian $H_{IIR}(f|f_c) = \frac{1}{1+(f/f_c)^2}$. $H_{IIR}(f|f_c)$ was estimated for each 30-min period as per the mean ambient relative humidity.

3.7 Linear regressions of ~~ET rates~~ latent heat fluxes from conventional- and low-cost eddy covariance

Results of a linear regression analysis between evapotranspiration rates obtained by the EC and EC-LC set-ups revealed a dependency of the evapotranspiration rates on the high-frequency cospectral correction method used. Evapotranspiration rates obtained by the EC-LC set-up using the Ibrom et al. (2007) high-frequency cospectral correction underestimated evapotranspiration rates obtained by EC using the high-frequency correction after Ibrom et al. (2007) (always used for the EC set-up) at all sites (Table 2). The largest underestimation was 32 % (Forst agroforestry) and the smallest underestimation was 13 % (Dornburg agroforestry), with a median underestimation of 22 % across all five plots.

In contrast, evapotranspiration estimates obtained by the EC-LC set-up using the Moncrieff et al. (1997) high-frequency cospectral correction revealed an underestimation of evapotranspiration rates by the EC-LC set-up of 14, 6, 5 and 1 % for the agroforestry plots of Reiffenhausen, Dornburg, Forst and Wendhausen, respectively, and an overestimation by the EC-LC set-up of 8 % for the monocultural agriculture plot of Dornburg ~~compared to conventional EC~~ relative to the conventional EC set-up (Table 2 and Fig. 11).

The dependency of the evapotranspiration estimates on the chosen high-frequency cospectral correction method may be caused by the assumptions of each method. The Ibrom et al. (2007) high-frequency correction method was initially developed for a closed-path eddy covariance system, with a tube length of about 50 m. The method described in Ibrom et al. (2007) takes into account the dependency of water vapour concentration measurements on relative humidity effects inside the tube. ~~Therefore, independent meteorological measurements of relative humidity and air temperature were required , when the method after Ibrom et al. (2007) was applied.~~ A low-pass cut-off frequency was estimated for each 30-min period as a function of ambient relative humidity. It is stated that at least one month of data were required to estimate the low-pass cut-off frequency (LI-COR, 2015).

~~The~~ In contrast, the high-frequency correction method after Moncrieff et al. (1997) is purely analytical and applies a fit of the temperature cospectra measured with the sonic anemometer on the water vapour cospectra. This analytical method can be applied independently of meteorological measurements. Furthermore, the correction after Moncrieff et al. (1997) was recommended for either open-path EC systems or under conditions when the intake tube is short and heated (LI-COR, 2015). From an analysis of the high-frequency transfer function from Moncrieff et al. (1997) and the Lorentzian of the infinite impulse response filter from Ibrom et al. (2007) it is evident that the correction of high-frequency losses is better represented by the high-frequency spectral correction of Moncrieff et al. (1997) (see Fig. 12). The transfer function after Moncrieff et al. (1997) is shifted towards higher frequencies and lower frequencies are conserved. According to the Lorentzian (Ibrom et al., 2007) the filtering properties are more pronounced for Ibrom et al. (2007) and low-frequencies ($<10^{-2}$ Hz) are attenuated. Based on the assumptions and recommendations given in Moncrieff et al. (1997) and LI-COR (2015), we decided to apply the correction of Moncrieff et al. (1997) to our EC-LC set-up.

2. RC: *Minor comments*

Abstract: I find the abstract too long, I am not sure though, if this journal has any limits in that respect. E.g. the introductory sentences could be shortened. Nevertheless, I would suggest to mention the main results, perhaps even including information about the RMSE.

2. AR: We shortened the Abstract as shown below.

Changes in the manuscript:

Abstract. ~~Eddy covariance has evolved as the method of choice for measurements of the ecosystem-atmosphere exchange of water vapour, sensible heat and trace gases. Under ideal conditions, eddy covariance provides direct and precise flux observations, commonly approximated from single point eddy covariance measurements. While eddy covariance is appropriate over uniform terrain of infinite extent, heterogeneous land surfaces compromise the representativity of single-point measurements as a predictor for ecosystem-wide fluxes and violate assumptions of the eddy covariance method. Therefore heterogeneous~~ Heterogeneous land surfaces require multiple measurement units for spatially adequate sampling and representative fluxes. The complexity and cost of traditional eddy covariance ~~instruments~~ set-ups typically limits the feasible number of sampling units. Therefore, new low-cost eddy covariance systems ~~are required~~ provide ideal opportunities for spatially replicated sampling~~, not only to increase the representativity of turbulent fluxes at a single site, but also for experiments where replication is required to e.g. compare different ecosystems~~.

The aim of this study was to test the performance of a compact low-cost pressure, temperature and relative humidity sensor for the application of evapotranspiration measurements by eddy covariance over agroforestry and conventional agriculture in Germany. We performed continuous low-cost eddy covariance measurements over agroforestry and conventional agriculture for reference, at five sites across Northern Germany over a period of two years from 2016 to 2017. We conducted side-by-side measurements using a roving enclosed-path eddy covariance set-up to assess the performance of the low-cost eddy covariance set-up.

Evapotranspiration measured with low-cost eddy covariance compared well with fluxes from conventional eddy covariance. ~~Diel cycles of evapotranspiration were well represented at a 30-min resolution. The differences between low-cost and conventional eddy covariance at 30-min resolution were small relative to the diel amplitude of the fluxes.~~ The slopes of linear regressions for evapotranspiration comparing low-cost and conventional eddy covariance set-ups ranged from 0.86 to 1.08 for five out of ten sites, indicating a 14% flux underestimation and a 8% flux overestimation relative to the conventional EC set-up, respectively. Corresponding coefficients of determination, R^2 ~~values~~, ranged from 0.71 to 0.94 across sites. ~~This indicates that a high proportion of the flux variability of the conventional eddy covariance set-up is reproduced by the low-cost eddy covariance set-up.~~ The root mean square error for differences between latent heat fluxes obtained by both set-ups were small compared to the overall flux magnitude, with a mean and standard deviation of 34.23 ± 3.2 W m^{-2}, respectively, across sites.

The spectral response characteristics of the low-cost eddy covariance set-up were inferior to the eddy covariance set-up in the inertial sub-range of the turbulent spectrum. The water vapour flux cospectrum of the low-cost eddy covariance set-up underestimated the theoretical slope of -4/3 stronger than the conventional eddy covariance set-up. This underestimation ~~is~~ was mainly caused by the limited response time of the low-cost thermohygrometer ~~of one second, which prevents eddies of a frequency higher than two times the response time to be adequately sampled by the thermohygrometer~~ longer than one second.

We conclude that low-cost eddy covariance sensors are an alternative to conventional eddy covariance sensors when ~~spatial~~, first, replicates are required ~~or when the scientific questions require a larger number of measurement units. An appropriately chosen high-frequency correction method is essential for the slow response sensor. The new low-cost eddy covariance set-up is a viable alternative, particularly when~~ and, second, the spatial variability of fluxes of the ecosystems of interest is larger than above reported set-up specific differences in fluxes.

3. RC: *P2, L10-21: It is not clear how this is relevant for the topic of this paper. Perhaps omit these sentences, although they are correct.*

3. AR: We shortened this paragraph and focused on the most important parts.

Changes in the manuscript:

~~particularly when~~ and, second, the spatial variability of fluxes of the ecosystems of interest is larger than above reported set-up specific differences in fluxes.

---

1 Introduction

Eddy covariance (EC) is often the method of choice for measurements of the ecosystem-atmosphere exchange of water vapour, sensible heat, momentum and trace gases (Baldocchi (2003), Baldocchi (2014), Farahani et al. (2007)) over a variety of ecosystems. ~~However, the EC method has a number of assumptions and is therefore only valid for measurements under stationary conditions, i.e. no change of the means of the scalar quantity with time (c.f. Taylor's hypothesis of frozen turbulence), over horizontally homogeneous terrain in the presence of a mean zero vertical velocity component and a negligible density flux (Foken and Wichura (1996), Kaimal et al. (2012)). Above conditions are rarely met over real ecosystems.~~

~~The concept of the flux footprint (Schmid, 2002) allows to relate the observed fluxes to a spatial region of the underlying surface. Position and extent of the footprint can be optimized to fit the target surface by adjusting tower position and measurement height, respectively. However, in heterogeneous landscapes, there are situations where the footprint from a single tower can not adequately capture the spatial variability of the underlying surface. This is often the case in agriculture landscapes with multiple crops and in spatially heterogeneous ecosystems. At sites with spatial variability of surface cover this can mean, depending on the footprint extent, that~~ At ecosystems with spatial variability of surface cover, the representativity of the measured fluxes is limited by the flux footprint extend (Schmid, 2002). Either the spatial variability of fluxes ~~can either remain~~ remains undetected (for small footprints) or can not be resolved explicitly (for large footprints). Such heterogeneous ecosystems require multiple towers for spatially representative flux sampling.

While the single-tower approach is still most common for ecosystem studies, a few studies have performed replicated EC measurements. Davis et al. (2010) studied carbon fluxes over an arable site in South East Ireland. Hollinger and Richardson (2005) used a set of two flux towers separated by a distance of 775 m for uncertainty estimation of EC flux measurements.

Replication of sampling points was traditionally limited by high costs and the complexity of conventional EC set-ups. Therefore, there is increasing interest in the development of low-cost sensors for different applications in the bio-geosciences.

Dias et al. (2007) proposed a cost-efficient direct attenuated EC set-up to measure latent heat fluxes, combining a sonic anemometer and a hygrometer of fast response. They applied a correction factor to the time-domain covariance between the vertical velocity and relative humidity measurements. Hill et al. (2017) presented a low-cost measuring set-up to measure both CO_2 and water vapour fluxes and discussed the value of increasing the number of measuring complexes for the statistical power of EC measurements in a variety of landscapes. Hill et al. (2017) concluded that at least four flux towers per site are required to confirm a statistical confidence of 95% that the flux over one year is not zero and therefore accept to a statistical confidence of 5% that the annual flux is zero. This is of major importance for an ecosystem, which is heterogeneous at a scale larger than the flux footprint of a single tower.

Besides the replication of measurement units within one ecosystem, the ecosystem-to-ecosystem replication of sampling points is of importance to e.g. assess the potential of forests for climate change mitigation and as a CO_2 sink (De Stefano and Jacobson, 2018). The outcome of synthesis studies, e.g. on the water use of terrestrial ecosystems at global scale (Tang et al., 2014) could be strengthened by an increased number of flux measuring units across ecosystems. Low-cost instrumentation can foster replicated EC measurements across the globe, especially in ecoregions that are currently only sparsely sampled, such as Africa, Oceania (except Australia) and South America (Hill et al. (2017) and Table 1 therein). With replicated measurements of low cost, effects of land-use changes or different agriculture management practices on turbulent fluxes can be assessed. A prominent example are flux measurements over heterogeneous shaped short rotation alley cropping systems (ACS) as one type of agroforestry (AF) in comparison to monocultural agriculture systems. Flux measurements over ~~ACSs~~ AFs require replicated measurements to capture the spatial variability of the turbulent fluxes both at a single ~~ACS~~ AF and across multiple ~~ACSs~~ AFs at different sites.

Our objectives are (a) to test the performance of a new EC measuring complex under field conditions to measure half-hourly evapotranspiration over ~~short rotation alley cropping~~ alley cropping agroforestry systems and monocultural agriculture systems, and (b) to evaluate the low-cost measuring complex relative to conventional EC instrumentation.

2 Material and Methods

2.1 Site description

The study is part of the SIGNAL (Sustainable intensification of Agriculture through agroforestry) project (http://www.signal.uni-goettingen.de/), which aims to evaluate the sustainability of agroforestry in Germany. It is based on data collected at five sites in Northern Germany (Fig. 1). Each site

4. RC: *L9, L7: How were the clocks of the two systems synchronized and how good was this synchronization. It needs to be better than 0.05 s.*

4. AR: We agree that this sentence was misleading. We changed the line accordingly. This sentence should rather be understood as matching of data sets. The turbulence data, the 3D wind and the sonic temperature, were sampled with a frequency of 20 Hz and the air temperature, relative humidity and air pressure were sampled with a frequency of 8 Hz on two data acquisition systems, the CR6 logger and the RaspberryPi, respectively. We matched the two different time stamps during preprocessing according to the nearest neighbour time stamp. Regarding the synchronization of the two different data acquisition systems, the time stamp of the RaspberryPi was synchronized hourly with an online ntp server, whereas the time on the CR6 logger was manually set during regular maintenance visits.

We corrected for a time lag between the 3D wind velocity and the sonic temperature recorded with the CR6 logger and the water vapour mole fraction recorded with the RaspberryPi during preprocessing, using the cross correlation function ccf (R-package ccf). We assume that the drift of the two acquisition systems is inside the window of the cross correlation function of 62.5 s.

Changes in the manuscript:

We ~~synchronized~~ matched the water vapour mole fraction calculated from the thermohygrometer data and the velocity components measured with the ultrasonic anemometer according to the nearest-neighbour date values to address the two different sampling frequencies of 8 Hz and 20 Hz, respectively. The two data acquisition systems (the CR6 logger and the RaspberryPi, respectively) were regularly manually synchronized. In detail, the RaspberryPi was synchronized with an online ntp server, whereas the CR6 logger was synchronized during regular maintenance visits.

5. RC: *P10, L17: Since you analyzed the spectra already, I suggest that you also empirically determine and present the cut-off frequency of the Bosch sensor, also in order to verify the response time provided in the specifications.*

5. AR: In the following we want to address the spectral response characteristics of the BME280 thermohygrometer in two ways, first, in terms of the cut-off frequency and as the derived sensor time constant and, second, in terms of the spectral correction factor for water vapour.

Changes in the manuscript:

1. cut-off frequency and sensor time constant

We included a new section (Section 3.4: Sensor cut-off frequency and time constant) on the sensors cut-off frequency and time constant into the manuscript and showed the dependency of the time constant on relative humidity (Figure 8).

3.4 Sensor cut-off frequency and time constant

The nominal time response of the relative humidity sensor as part of the thermohygrometer yields a theoretical sensor cut-off frequency of 0.16 Hz (6.3 s) calculated from Eq. 13.

Under field conditions we observed a mean cut-off frequency of 0.063 ± 0.02 Hz for the low-cost thermohygrometer and 0.3 ± 0.2 Hz for the LI-7200 gas analyser across five plots and all humidity classes (from 30 % to 90 % relative humidity bins). The respective mean time constant was 2.8 ± 1 s for the low-cost thermohygrometer and 0.6 ± 0.3 s for the LI-7200 gas analyser (see Fig. 8). For both sensors we found an exponential increase of the time constant with relative humidity (see Fig. 8).

Under field conditions, the cut-off frequency and the respective time constant of the thermohygrometer were inferior to the one given in the specifications. We interpret this as caused by the design of the enclosure. The thermohygrometer is placed at the end of a cylinder with the ventilator directly below, so that the flow velocity is decelerated. Subsequently, the decelerated flow velocity leads to a limited signal response. One suggestion for improvement of the frequency response would be to place

the thermohygrometer inside a longer tube with a fre moving air stream. This ensures a faster air exchange ins the measurement cell of the thermohygrometer and henc faster response time.

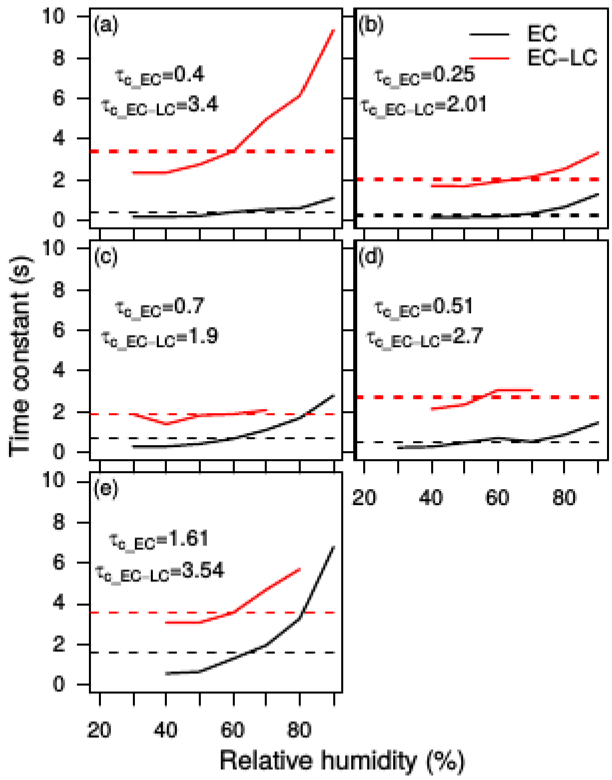

Figure 8. Time constant against relative humidity for the LI-7200 (black solid lines) and the thermohygrometer (red solid lines). Dashed lines with the same colour coding as for data shown and values written, correspond to the mean time constant for the respective sensors across all relative humidity classes. Sites correspond to Dornburg agroforestry, (a), Dornburg monoculture, (b), Forst agroforestry, (c), Reiffenhausen agroforestry, (d), and Wendhausen agroforestry, (e).

2. spectral correction factor for water vapour

Site	Spectral correction factor (-)		Spectral correction factor flux magnitude change (%)	
Method	**EC**	**EC-LC**	**EC**	**EC-LC**
Dornburg AF	1.11	1.76	6.9	40.82
Dornburg MC	1.21	3.01	14.3	60.9
Forst AF	1.1	1.99	9.9	47.7
Reiffenhausen AF	1.11	1.31	9.4	42.3
Wendhausen AF	1.16	1.74	5.9	21.83
Mean+-sd	**1.14** ±0.05	**1.962** ±0.64	**9.28** ±3.3	**42.7** ±14.1

Table 1: Median spectral correction factor and the impact of the spectral correction factor on the flux magnitude change.

We found a higher frequency correction factor for water fluxes (combines the correction for high and low-frequency losses) obtained by the EC-LC set-up than for the EC set-up with a median flux increase of 97.4% and 14.6% (see Table 1 and Figure 6 a), respectively.

The effect of the spectral corrections on a flux magnitude increase was most pronounced for the low-cost set-up than for the conventional EC set-up with an overall flux magnitude increase of 42.7 ±14.1 % and 9.28 ±3.3 % for the EC-LC and the EC set-up, respectively (see Figure 3 and Table 1 of the current document).

We found the highest median spectral correction factor (3.01) and the highest flux magnitude increase (60.9%) caused by the high-frequency correction for the low-cost set-up of the monocultural agriculture plot of Dornburg. We interpret the higher spectral correction factor as caused by different measurement heights, with a measurement height of 3.5 m at the monocultural agriculture plot of Dornburg and a measurement height of 10 m at the agroforestry plot of Dornburg. At the lower tower high frequency eddies are more likely than at the taller tower. As the nominal time response (1 s) given in the specifications and the estimated time response are quite low, the flux loss is high and needs to be corrected for.

We included information on the spectral correction factor into Section 3.3 (“Effect of spectral- and WPL corrections on evapotranspiration rates from low-cost eddy covariance”) and Figure 6 into the manuscript.

The high-frequency correction after Moncrieff et al. (1997) accounted for 23 % of the fully corrected flux, which was the largest contribution of all corrections to a flux magnitude increase. We interpret the high contribution of the correction from Moncrieff et al. (1997) as a result of the low response time of the thermohygrometer. In ~~a study by Ibrom et al. (2007) ,~~ Ibrom et al. (2007) the low-pass filtering properties of the closed-path system led to an underestimation of the measured latent heat flux and resulted in a necessary correction of 42 %.

The overall impact of spectral corrections on a change of the turbulent latent heat fluxes was stronger for the EC-LC set-up compared to the EC set-up. Here, we quantify the overall impact of spectral corrections on latent heat fluxes in terms of the spectral correction factor (SCF) calculated for each 30-minute period. The 30-minute SCF was multiplied with the respective uncorrected flux. A SCF larger than one indicates a flux magnitude increase, whereas a SCF lower than one indicates a flux magnitude decrease. Box-whisker plots of 30-minute SCFs for each site and each set-up are shown in Figure 7 (a). We found a mean SCF of 1.96 ± 0.64 for the EC-LC set-up and 1.14 ± 0.05 for the EC set-up across all sites, indicating a mean flux magnitude increase of 96 % for the EC-LC set-up and a mean flux magnitude increase of 14 % for the EC set-up. The mean SCF presented here integrates both night and day time periods. Thus, a high SCF during night time with commonly low latent heat fluxes leads to a smaller change of the flux magnitude than during day time, when fluxes are commonly high. Therefore, we also present the sum of 30-minute ET rates corrected for spectral losses and the sum of the total ET attributed to the spectral corrections in Figure 7 (b). The part of the total corrected ET attributed to the spectral corrections was higher for the EC-LC set-up compared to the EC-set-up and amounted on average to 42.7 ± 14.1 % of total ET for the EC-LC set-up and 9.3 ± 3.3 % of total ET for the EC set-up.

Across sites, we found the highest median spectral correction factor of 3.01 and the highest part of the total corrected ET attributed to the spectral corrections of 60.9 % for the EC-LC set-up at the monocultural agriculture plot of Dornburg. We interpret this as a measurement height dependency of the spectral corrections. The measurement height at the agroforestry plots was 10 m and at the monocultural agriculture plots the measurement height was 3.5 m. We assume that high-frequency eddies are more likely close to the surface. Therefore, a detected turbulent signal at the lower measurement height would be shifted towards high frequencies compared to the detected turbulent signal at the higher measurement height (Aubinet et al., 2012). If a sensor is not capable of detecting the turbulent signal in the high frequency range of the spectrum, the signal is attenuated and needs to be corrected.

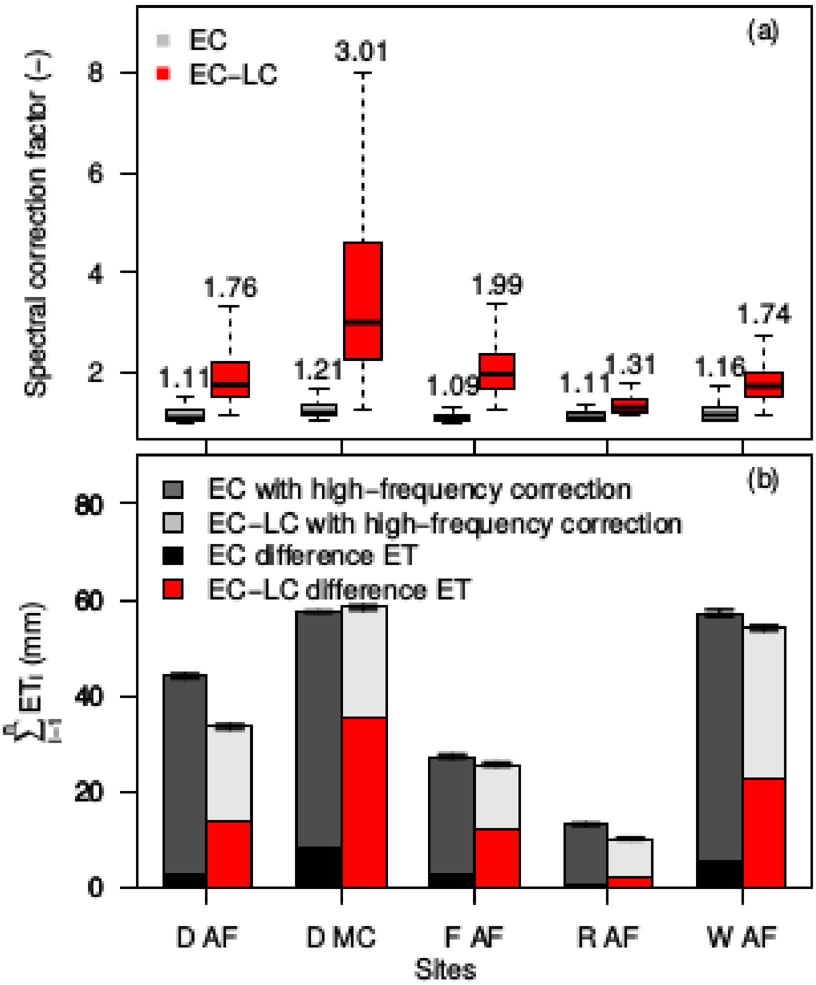

Figure 6. a) Box-whisker plot of spectral correction factors for the EC (grey) and the EC-LC (red) set-up for all sites. Values above the bars correspond to the median spectral correction factor, and, b) cumulative evapotranspiration rates for the EC and EC-LC set-ups for all sites, e.g Dornburg agroforestry, (D AF), Dornburg monoculture, (D MC), Forst agroforestry, (F AF), Wendhausen agroforestry, (W AF), and Reiffenhausen agroforestry, (R AF), over the respective campaign periods (Table A2). The error bars in Figure (b) correspond to the summed random uncertainties. The black and red bars correspond to that part of the total ET attributed to the high-frequency correction for the EC and EC-LC set-up, respectively. Incomplete records with either of EC or EC-LC missing were omitted.

Low-cost eddy covariance: a case study of evapotranspiration over agroforestry in Germany

Christian Markwitz[1] **and Lukas Siebicke**[1]

[1]Bioclimatology, University of Goettingen, Büsgenweg 2, 37077 Göttingen, Germany

Correspondence to: Christian Markwitz (christian.markwitz@forst.uni-goettingen.de)

Abstract. ~~Eddy covariance has evolved as the method of choice for measurements of the ecosystem-atmosphere exchange of water vapour, sensible heat and trace gases. Under ideal conditions, eddy covariance provides direct and precise flux observations, commonly approximated from single point eddy covariance measurements. While eddy covariance is appropriate over uniform terrain of infinite extent, heterogeneous land surfaces compromise the representativity of single-point measurements as a predictor for ecosystem-wide fluxes and violate assumptions of the eddy covariance method. Therefore heterogeneous~~ Heterogeneous land surfaces require multiple measurement units for spatially adequate sampling and representative fluxes. The complexity and cost of traditional eddy covariance ~~instruments~~ set-ups typically limits the feasible number of sampling units. Therefore, new low-cost eddy covariance systems ~~are required~~ provide ideal opportunities for spatially replicated sampling~~, not only to increase the representativity of turbulent fluxes at a single site, but also for experiments where replication is required to e.g. compare different ecosystems~~.

The aim of this study was to test the performance of a compact low-cost pressure, temperature and relative humidity sensor for the application of evapotranspiration measurements by eddy covariance over agroforestry and conventional agriculture in Germany. We performed continuous low-cost eddy covariance measurements over agroforestry and conventional agriculture for reference, at five sites across Northern Germany over a period of two years from 2016 to 2017. We conducted side-by-side measurements using a roving enclosed-path eddy covariance set-up to assess the performance of the low-cost eddy covariance set-up.

Evapotranspiration measured with low-cost eddy covariance compared well with fluxes from conventional eddy covariance. ~~Diel cycles of evapotranspiration were well represented at a 30-min resolution. The differences between low-cost and conventional eddy covariance at 30-min resolution were small relative to the diel amplitude of the fluxes.~~ The slopes of linear regressions for evapotranspiration comparing low-cost and conventional eddy covariance set-ups ranged from 0.86 to 1.08 for five out of ten sites, indicating a 14% flux underestimation and a 8 % flux overestimation relative to the conventional EC set-up, respectively. Corresponding coefficients of determination, R^2~~values ,~~, ranged from 0.71 to 0.94 across sites. ~~This indicates that a high proportion of the flux variability of the conventional eddy covariance set-up is reproduced by the low-cost eddy covariance set-up.~~ The root mean square error for differences between latent heat fluxes obtained by both set-ups were small compared to the overall flux magnitude, with a mean and standard deviation of 34.23 ± 3.2 W m^{-2}, respectively, across sites.

The spectral response characteristics of the low-cost eddy covariance set-up were inferior to the eddy covariance set-up in the inertial sub-range of the turbulent spectrum. The water vapour flux cospectrum of the low-cost eddy covariance set-up underestimated the theoretical slope of -4/3 stronger than the conventional eddy covariance set-up. This underestimation ~~is~~ was mainly caused by the limited response time of the low-cost thermohygrometer ~~of one second, which prevents eddies of a frequency higher than two times the response time to be adequately sampled by the thermohygrometer~~longer than one second.

We conclude that low-cost eddy covariance sensors are an alternative to conventional eddy covariance sensors when~~spatial~~ , first, replicates are required ~~or when the scientific questions require a larger number of measurement units. An appropriately chosen high-frequency correction method is essential for the slow response sensor. The new low-cost eddy covariance set-up is a viable alternative,~~

~~particularly when~~ and, second, the spatial variability of fluxes of the ecosystems of interest is larger than above reported set-up specific differences in fluxes.

---

1 Introduction

Eddy covariance (EC) is often the method of choice for measurements of the ecosystem-atmosphere exchange of water vapour, sensible heat, momentum and trace gases (Baldocchi (2003), Baldocchi (2014), Farahani et al. (2007)) over a variety of ecosystems. ~~However, the EC method has a number of assumptions and is therefore only valid for measurements under stationary conditions, i.e. no change of the means of the scalar quantity with time (c.f. Taylor's hypothesis of frozen turbulence), over horizontally homogeneous terrain in the presence of a mean zero vertical velocity component and a negligible density flux (Foken and Wichura (1996), Katul et al. (2012)). Above conditions are rarely met over real ecosystems .~~

~~The concept of the flux footprint (Schmid, 2002) allows to relate the observed fluxes to a spatial region of the underlying surface. Position and extent of the footprint can be optimized to fit the target surface by adjusting tower position and measurement height, respectively. However, in heterogeneous landscapes, there are situations where the footprint from a single tower can not adequately capture the spatial variability of the underlying surface. This is often the case in agriculture landscapes with multiple crops and in spatially heterogeneous ecosystems. At sites with spatial variability of surface cover this can mean, depending on the footprint extent, that~~ At ecosystems with spatial variability of surface cover, the representativity of the measured fluxes is limited by the flux footprint extend (Schmid, 2002). Either the spatial variability of fluxes ~~can either remain~~ remains undetected (for small footprints) or can not be resolved explicitly (for large footprints). Such heterogeneous ecosystems require multiple towers for spatially representative flux sampling.

While the single-tower approach is still most common for ecosystem studies, a few studies have performed replicated EC measurements. Davis et al. (2010) studied carbon fluxes over an arable site in South East Ireland. Loescher et al. (2017) used a set of two flux towers separated by a distance of 775 m for uncertainty estimation of EC flux measurements.

Replication of sampling points was traditionally limited by high costs and the complexity of conventional EC set-ups. Therefore, there is increasing interest in the development of low-cost sensors for different applications in the biogeosciences.

Dias et al. (2007) proposed a cost-efficient direct attenuated EC set-up to measure latent heat fluxes, combining a sonic anemometer and a hygrometer of fast response. They applied a correction factor to the time-domain covariance between the vertical velocity and relative humidity measurements. Hill et al. (2017) presented a low-cost measuring set-up to measure both CO_2 and water vapour fluxes and discussed the value of increasing the number of measuring complexes for the statistical power of EC measurements in a variety of landscapes. Hill et al. (2017) concluded that at least four flux towers per site are required to confirm a statistical confidence of 95 % that the flux over one year is not zero and therefore accept to a statistical confidence of 5% that the annual flux is zero. This is of major importance for an ecosystem, which is heterogeneous at a scale larger than the flux footprint of a single tower.

Besides the replication of measurement units within one ecosystem, the ecosystem-to-ecosystem replication of sampling points is of importance to e.g. assess the potential of forests for climate change mitigation and as a CO_2 sink (De Stefano and Jacobson, 2018). The outcome of synthesis studies, e.g. on the water use of terrestrial ecosystems at global scale (Tang et al., 2014) could be strengthened by an increased number of flux measuring units across ecosystems. Low-cost instrumentation can foster replicated EC measurements across the globe, especially in ecoregions that are currently only sparsely sampled, such as Africa, Oceania (except Australia) and South America (Hill et al. (2017) and Table 1 therein). With replicated measurements of low cost, effects of land-use changes or different agriculture management practices on turbulent fluxes can be assessed. A prominent example are flux measurements over heterogeneous shaped short rotation alley cropping systems (ACS) as one type of agroforestry (AF) in comparison to monocultural agriculture systems. Flux measurements over ~~ACSs~~ AF require replicated measurements to capture the spatial variability of the turbulent fluxes both at a single ~~ACS~~ AF system and across multiple ~~ACSs at different sites~~AF systems.

Our objectives are (a) to test the performance of a new EC measuring complex under field conditions to measure half-hourly evapotranspiration over ~~short rotation alley cropping~~ alley cropping agroforestry systems and monocultural agriculture systems, and (b) to evaluate the low-cost measuring complex relative to conventional EC instrumentation.

2 Material and Methods

2.1 Site description

The study is part of the SIGNAL (Sustainable intensification of Agriculture through agroforestry) project (http://www.signal.uni-goettingen.de/), which aims to evaluate the sustainability of agroforestry in Germany. It is based on data collected at five sites in Northern Germany (Fig. 1).

Each site consists of an agroforestry (AF)- and a ~~control plot~~monocultural control plot (MC). The agroforestry plots are alley cropping systems, consisting of fast growing trees, such as willow [*Salix*], poplar [*Populus*] and black locust [*Robinia*], interleaved by either annually rotating crops or perennial grassland. The control plots consist of the same crop or grass type as planted between the tree strips and are managed as monocultural agriculture~~(MC)~~. Three sites undergo annual crop rotation (Dornburg, Forst and Wendhausen), while two systems are of a perennial grassland type (Mariensee and Reiffenhausen). The project design includes a fixed tree alley width of 10 m, while alley length and number are variable across sites. Tree alley distances vary between 10 m, 24 m, 48 m and 96 m. The area covered by trees in relation to the whole agroforestry plot area varies between 6~~%~~ % and 72~~% (~~ %. Table A1 provides an overview of site locations~~and agroforestry geometry).~~ , agroforestry geometry and stand characteristics.

We performed a flux footprint climatology analyses with the flux footprint prediction online tool (http://footprint.kljun.net/, Kljun et al. (2015)). The flux footprint climatology is valid for the respective campaign and only for daytime data according to a global radiation $R_G > 20\ \mathrm{W\,m^{-2}}$. We found a 90 % flux magnitude contribution of the agroforestry plot of Forst and the monoculture plot of Dornburg and a 80% flux magnitude contribution of the agroforestry plots of Dornburg and Wendhausen. The smallest agroforestry system of Reiffenhausen contributed the least to the measured turbulent flux with 60 %. Outside the agroforestry plot, fluxes were affected by nearby crop fields in about 400 m distance to the flux tower in northerly direction and forest in about 200 m distance in southerly direction.

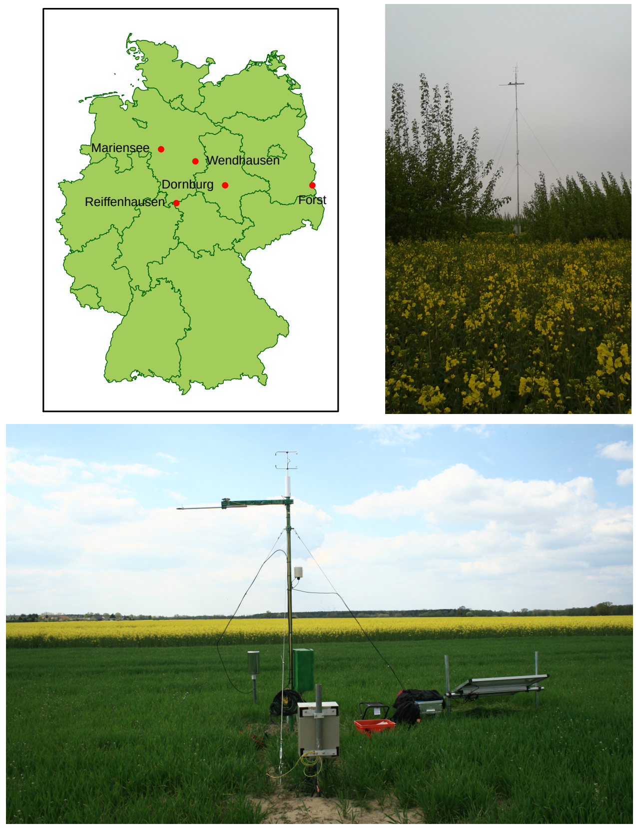

Figure 1. Top left: SIGNAL sites (Map source: Bundesamt für Kartographie und Geodäsie (2011)); top right: agroforestry plot in Dornburg with eddy covariance mast; bottom: monocultural agriculture plot in Forst (Lower Lusatia) with eddy covariance mast.

2.2 Instrumental set-up

2.2.1 Standard meteorological measurements

Continuous measurements of micrometeorological and standard meteorological variables were performed since March 2016. At each agforestry plot one eddy covariance mast with a height of 10 m was installed and at each monocultural plot one eddy covariance mast with a height of 3.5 m. Each mast at the agroforestry and the monocultural plot was equipped with an identical instrumental set-up. An overview of all installed instruments is given in Table 1. The data were logged and stored on a CR6 data logger (*Campbell Scientific*, Inc., Logan, UT, USA). The meteorological data were regularly sent to a database via mobile phone network.

2.2.2 Conventional eddy covariance installation

Fluxes of sensible heat and momentum were continuously measured with a uSONIC3-omni (*METEK GmbH*, Elmshorn, Germany) ultrasonic anemometer. CO_2 and water vapour fluxes were measured in campaigns during the vegetation periods of 2016 and 2017. During the 2016 campaign, fluxes were measured during two consecutive periods of four weeks duration separately at the agroforestry and monocultural plots, whilst in 2017 both plots were sampled simultaneously over a time period of approximately four weeks (see Table A2 for exact dates). During the campaigns, the instrumentation specified in Table 1 was complemented by a LI-7200 (*LI-COR Inc.*, Lincoln, Nebraska, USA) enclosed-path infrared gas analyser (Burba et al., 2012). The data were measured together with the three-dimensional wind velocity and the sonic temperature and stored on the same data logger (CR6 , *Campbell Scientific Ltd.*, Bremen, Germany) as used for the meteorological variables. The water vapour and CO_2 mole fractions were sampled with a sampling frequency of 20 Hz. The intake tube was of 1 m length and had an inner tube diameter of 5.3 mm (2016) and 8.2 mm (2017). The separation ~~between the intake tube and~~ of the gas analysers intake tube relative to the centre of the sonic anemometer was different for each plot and is summarized in Table A3. The flow rate was kept constant at 15 slpm.

Table 1. Instrumentation for flux and meteorological measurements used at all five agroforestry and five monocultural agriculture plots.

Variable	Height [m]	Instrument	Company
Standard meteorological measurements			
3D wind components, u, v, w, sonic temperature, T_s, wind speed and -direction	3.5,10	uSONIC-3 Omni	METEK GmbH, Elmshorn, Germany
Net radiation, R_N	3, 9.5	NR-Lite2 Net Radiometer	Kipp&Zonen, Delft, The Netherlands
Global radiation, R_G	3, 9.5	CMP3 Pyranometer	Kipp&Zonen, Delft, The Netherlands
Relative humidity, RH, air temperature, T	2	Hygro-Thermo Transmitter-compact (Model 1.1005.54.160)	Thies Clima, Göttingen, Germany
Precipitation	1	Precipitation Transmitter (Model 5.4032.35.007)	Thies Clima, Göttingen, Germany
Atmospheric pressure, ppp	0.5	Baro Transmitter (Model 3.1157.10.000)	Thies Clima, Göttingen, Germany
Ground heat flux, G	-0.05	Hukseflux HFP01	Hukseflux, Delft, The Netherlands
Soil temperature, T_{Soil}	-0.02, -0.05, -0.10, -0.25, -0.5	DS18B20	
Conventional eddy covariance measurements			
u, v, w, T_s	3.5,10	uSONIC-3 Omni	METEK GmbH, Elmshorn, Germany
Water vapour mole fraction, $C_{H_2O_v}$	3.5, 10	LI-7200	LI-COR Inc., Lincoln, Nebraska (USA)
Carbon dioxide mole fraction, C_{CO_2}	3.5, 10	LI-7200	LI-COR Inc., Lincoln, Nebraska (USA)
Low-cost eddy-covariance measurements			
u, v, w, T_s	3.5,10	uSONIC-3 Omni	METEK GmbH, Elmshorn, Germany
RH, T, ppp	3,9.5	BME280	Robert Bosch GmbH, Stuttgart, Germany

2.2.3 Low-cost eddy-covariance (EC-LC) installation

The low-cost eddy-covariance set-up ~~comprised of~~ shared the same ultrasonic anemometer (uSONIC3-omni) as used for the conventional EC ~~method and a~~ set-up. The water vapour mole fraction was derived from the combined digital pressure, relative humidity and air temperature sensor ~~(~~BME280 ~~,~~ manufactured by *Robert Bosch GmbH*, Stuttgart, Germany ~~) (Fig. 2)~~(hereafter named thermohygrometer). Figure 2 depicts the low-cost set-up. The measuring principle of the air pressure sensor is resistive, for the relative humidity sensor capacitive and for the temperature sensor is based on diode voltage measurements. The ultrasonic anemometer measured the three-dimensional wind speed and the ultrasonic temperature at a frequency of 20 Hz, whereas the thermohygrometer measured the air temperature, relative humidity and air pressure at a sampling frequency of 8 Hz. The specified response time of the thermohygrometer for relative humidity measurements is 1 s to overcome 63% of a step change from 90% to 0% or 0% to 90~~relative humidity .~~% relative humidity at 25 °C air temperature.

The response time of the temperature sensor of the thermohygrometer was not explicitly stated. Therefore, we estimated the response time in a lab experiment. We exposed the temperature sensor to a rapid temperature change about 10 °C warmer than ambient air temperature. The time constant τ was then directly proportional to the slope of the linear regression fit

$$t = \tau \ln\left(\frac{\vartheta(t=1) - \vartheta_{Ambient}}{\vartheta(t=t_{var}) - \vartheta_{Ambient}}\right)$$

with the measurement time, t, the air temperature at the first time step, $\vartheta(t=1)$, the ambient air temperature, $\vartheta_{Ambient}$, and air temperature at variable time step, $\vartheta(t=t_{var})$. The time constant achieved for the temperature sensor was 23.3±0.9 s as a mean of four replications. During the lab experiment the thermohygrometer was placed inside the same housing as deployed in the field.

The thermohygrometer was placed 0.5 m below the centre of the sonic anemometer in a PVC housing to protect the thermohygrometer from precipitation. ~~A~~ The PVC housing consisted of an outer and an inner cylinder. The inner cylinder was perforated on the top to provide a continuous air flow of 15 lpm, generated by a ventilator (HA30101V3-0000-A99, *Sunonwealth Electric Machine Industry Co. Ltd.*, Fresnes Cedex, France). The ventilator was placed below the thermohygrometer ~~provided a continuous air flow of 15~~inside the inner cylinder. The volume of the inner cylinder was 98.1 ~~lpm.~~ cm^3.

The absolute accuracy tolerance of the ~~thermohygrometer~~ relative humidity sensor was specified as ± 3~~relative humidity (Bosch Sensortec GmbH, 2016). Data~~ % for 20 % to 80 % relative humidity at 25 $°C$ air temperature. For the temperature sensor an absolute accuracy tolerance of $\pm 0.5\,°C$ at 25 $°C$ air temperature was given and for a temperature range of 0 $°C$ to 65 $°C$ an absolute accuracy tolerance of $\pm 1\,°C$ was specified. The pressure sensor has an absolute accuracy tolerance of ± 1 hPa for a pressure range from 300 hPa to 1100 hPa at air temperature between 0 $°C$ and 65 $°C$ (Bosch Sensortec GmbH, 2016).

Digital data from the thermohygrometer were recorded via the i2c protocol and stored on a RaspberryPi model B+ (*Raspberry Pi Foundation*, Cambridge, UK). The thermohygrometer has very low power consumption of approximately 3.6 μA at a sampling frequency of 1 Hz. The power draw of the thermohygrometer is 9.4e-5 W at a measuring frequency of 8 Hz, if powered with 3.3 V and if all three variables are measured at the same time. The RaspberryPi has a maximum power consumption of about 1.1 W.

The potential of the low-cost EC set-up are replicated measurements of evapotranspiration across different ecosystems. The relative cost of the low-cost set-up (featuring a sonic anemometer, a RaspberryPi and the thermohygrometer of low cost) is often less then 10 % of a typical conventional EC set-up. Beside a precipitation protection and a stable power supply, the thermohygrometer needs low maintenance. The mean time before failure of the sensor in our study was approximately 2 years.

2.3 Flux computation

2.3.1 Conventional eddy covariance set-up

Latent heat fluxes and sensible heat fluxes were calculated with the open source EddyPro® eddy covariance software (*LI-COR, Inc.*, Lincoln, Nebraska, USA, version 6.2.0).

The fluxes were computed as

$$H = \rho_a c_p \overline{w'T_s'} \tag{1}$$

$$\lambda E_{EC} = \lambda M_{H_2O_v} \overline{w' d'_{H_2O_v}} \tag{2}$$

with the density of dry air, ρ_a, the specific heat capacity at constant pressure, c_p, the vertical velocity component, w, the ultrasonic temperature, T_s, the latent heat of evaporation, λ, the molar mass of water vapour, $M_{H_2O_v}$, and the molar density of water vapour, $d_{H_2O_v}$. Primes denote deviations from the mean and overlines denote time averages.

Fluxes were calculated over a block averaging period of 30 minutes. The horizontal wind component was rotated into the mean wind direction via double rotation (Kaimal and Finnigan, 1994). Time lags between the ultrasonic anemometer and the intake tube of the LI-7200 gas analyser were calculated and corrected as a function of relative humidity (LI-COR, 2015). The effect of density fluctuations on the turbulent fluxes was corrected for by the WPL correction (Webb et al., 1980) and the ultrasonic temperature was corrected for humidity effects (Schotanus et al., 1983). Fluxes of sensible and latent heat, and momentum were filtered by removing all flux values corresponding to a flag of 2, following the two-stage quality control procedure of Mauder and Foken (2011b). Latent heat fluxes below -50 $W\,m^{-2}$ and above 500 $W\,m^{-2}$ were discarded. We further discarded latent heat fluxes according to the 97.5 % percentile of the H_2O variance and spikes were removed after Vickers and Mahrt (1997). Through quality check 9.6 ± 3.2 % of half-hourly latent heat fluxes obtained by the EC set-up were discarded and 10.4 ± 3.8 % of half-hourly latent heat fluxes obtained by the EC-LC set-up were discarded, as a mean over all five plots. Low-frequency and high-frequency losses were corrected by the procedure of Moncrieff et al. (2004) and Ibrom et al. (2007), respectively. Random uncertainties of ~~the latent heat~~ fluxes were calculated after Mann and Lenschow (1994).

Figure 2. Low-cost eddy covariance instrumentation, featuring a uSONIC3-omni sonic anemometer and a BME280 thermohygrometer. The thermohygrometer is placed in a ventilated PVC housing below the sonic anemometer.

2.3.2 Low-cost eddy covariance set-up

The latent heat flux from the low-cost eddy covariance set-ups was calculated as the covariance between the vertical velocity and the water vapour mole fraction, again with the EddyPro® eddy covariance software (*LI-COR, Inc.*, Lincoln, Nebraska, USA, version 6.2.0). The water vapour mole fraction, $C_{H_2O_v}$, was derived from relative humidity, temperature and pressure measured with the thermohygrometer from the definition of the specific humidity, q, as the quantity of water vapour per quantity of moist air. The latter two quantities were expressed as the density of water vapour, $\rho_{H_2O_v}$, and moist air, ρ_m, respectively. The density of moist air is defined as the sum of the density of dry air, ρ_d, and the density of water vapour.

$$\begin{aligned} q &= \frac{\rho_{H_2O_v}}{\rho_m} \\ &= \frac{\rho_{H_2O_v}}{\rho_d + \rho_{H_2O_v}} \end{aligned} \tag{3}$$

We then replaced the density of water vapour and the density of dry air in Eq. (3) as per Eqs. (4) and (5), respectively,

$$\rho_{H_2O_v} = \frac{C_{H_2O_v} \cdot M_{H_2O_v}}{V_m} \tag{4}$$

$$\rho_d = \frac{p - e}{R_d \cdot T_A} \tag{5}$$

with the molar mass of water vapour, $M_{H_2O_v} = 18.02\,\mathrm{g\,mol^{-1}}$, the molar volume of air

$$V_m = \frac{\Re \cdot T_A}{p}\,(m^3\,mol^{-1}), \tag{6}$$

the universal gas constant, $\Re = 8.314\,\mathrm{J\,mol^{-1}K^{-1}}$, and the specific gas constant of dry air, $R_d = 287.058\,\mathrm{J\,kg^{-1}\,K^{-1}}$.

Solving Eq. (3) for $C_{H_2O_v}$ leads to the water vapour mole fraction

$$C_{H_2O_v} = \frac{q\,\Re\,(p - e)}{p\,M_{H_2O}\,R_d(1 - q)}. \tag{7}$$

The specific humidity in Eq. (7) was calculated as a function of relative humidity, temperature and air pressure measurements from the thermohygrometer:

$$q = 0.622 \cdot \frac{e}{p} \tag{8}$$

The saturation vapour pressure, E_{Sat}, and vapour pressure, e, in Eq. (8) were calculated using Eqs. (11) and (12), respectively.

The water vapour mole fraction is expressed as the wet mole fraction, thus the mass of water vapour molecules per total mass of air. Therefore, latent heat fluxes derived from the water vapour mole fraction needs to be corrected for density effects (WPL correction, Webb et al. (1980)) caused by temperature and water vapour fluctuations. The WPL correction requires true ambient air temperature measurements. Our fast measurements of the true air temperature obtained by the thermohygrometer were attenuated by the slow response time of the ~~thermohygrometer (see Fig. ?? (b))~~thermohygrometers temperature measurements. Additionally, the air temperature obtained by the thermohygrometer overestimated the ultrasonic temperature used as a reference ~~(see Fig. ?? (c))~~ caused by a radiation effect from the grey PVC housing. ~~We therefore~~ Therefore, we derived a true air temperature for the WPL correction from the definition of the ultrasonic temperature, T_s, and its dependency on air humidity

$$T_s = T\,(1 + 0.32\frac{e}{p}) \tag{9}$$

with the atmospheric pressure, p, to calculate a moisture corrected temperature, which we used as an estimate of true air temperature, T:

$$T = \frac{T_s}{(1 + 0.32\frac{e}{p})} \tag{10}$$

An initial value for the vapour pressure in Eq. (10) was calculated from an approximation of the saturation vapour pressure, E_{Sat} (based on T_s) (Stull, 1989) and from relative humidity, *RH*,

$$E_{Sat} = 0.6112 \exp \frac{17.6294 \cdot (T_s - 273.16)}{T_s - 35.86K} \tag{11}$$

$$e = \frac{RH \cdot E_{Sat}}{100} \tag{12}$$

The derivation of the vapour pressure was iterated using Eqs. (9), (10), and (11).

We ~~synchronized~~ matched the water vapour mole fraction calculated from the thermohygrometer data and the velocity components measured with the ultrasonic anemometer according to the nearest-neighbour date values to address the two different sampling frequencies of 8 Hz and 20 Hz, respectively. The two data acquisition systems (the CR6 logger and the RaspberryPi, respectively) were regularly manually synchronized. In detail, the RaspberryPi was synchronized with an online ntp server, whereas the CR6 logger was synchronized during regular maintenance visits.

A timelag ~~caused by the vertical separation of about 0.5 m~~ between the anemometer and the thermohygrometer was corrected for in a preprocessing routine. The cross-correlation function *ccf* from the R-package ~~tseries~~ *tseries* (Trapletti and Hornik, 2017) was used to detect the timelag between the vertical velocity component and the water vapour mole fraction. The respective timelag was extracted according to the maximum cross-correlation coefficient. The estimated lag time was used to merge the velocity components, u, v~~and~~, w, and the ultrasonic temperature with the nearest-neighbour water vapour mole fraction.

We applied the same ~~corrections for the flux computation to~~ flux corrections and quality checks to fluxes obtained by the EC-LC set-up as for the conventional EC ~~method~~ set-up (see Sect. 2.3.1). The only difference was the correction of high-frequency losses, where we applied the correction after Moncrieff et al. (1997). The correction procedure was explicitly recommended by Moncrieff et al. (1997) for either open-path sensors or closed-path systems of very short and heated sampling lines.

The method is fully ~~analytical~~ analytic and for each half-hour period the flux cospectra are estimated from analytical formulations after Moncrieff et al. (1997) (Eqs. (12)-(18) therein). Those equations are a modified version of the formulas in Kaimal et al. (1972). The cospectra are expressed as a function of the normalized frequency, which is a function of the natural frequency, measurement height, zero displacement height, wind speed and atmospheric stability.

We studied the impact of the different corrections on the raw turbulent evapotranspiration rates, obtained by the EC-LC set-up. We applied the single corrections separately on a test data-set from the agroforestry plot in Dornburg from the 14-July to the 12-August, 2016. We assessed the impact of the following corrections on the raw evapotranspiration rates: 1) the fully analytic high-frequency cospectral correction after Moncrieff et al. (1997), 2) the low-frequency cospectral correction after Moncrieff et al. (2004) and 3) the WPL correction after Webb et al. (1980). The corresponding results are presented in Sect. 3.3.

Linear regression analyses were performed between evapotranspiration obtained by the EC ~~method~~ set-up and the EC-LC set-up. We used the major axis linear regression method from the *lmodel2* function as part of the lmodel2 R-package (Legendre and Oksanen, 2018). The major axis linear regression method assumes equally distributed errors in both time series.

2.4 Spectral analysis

Commonly, high-frequency trace gas measurements (e.g. the water vapour- or CO_2 mole fraction) taken by closed- or enclosed-path gas analysers are attenuated in the high-frequency range of the energy spectrum (Lenschow and Raupach, 1991). Attenuation is mainly caused by exchange processes (adsorption or desorption) of gas molecules with tubing walls (Leuning and Moncrieff (1990), Ibrom et al. (2007)). This effect is most severe for sticky gases such as water vapour. In contrast, the temperature spectrum and cospectrum is assumed to be not attenuated by the molecular exchange processes with tubing walls, as the measurements are taken with a sonic anemometer, which is open-path. Attenuation of the ultrasonic temperature and the wind velocity components is mainly caused by the path-averaging effect, especially at low wind speeds and at very high wavenumbers (Kristensen and Fritzjarrals, 1984), which is outside the inertial sub-range. Therefore, we quantified the frequency response characteristics of the ~~conventional~~ EC- and EC-LC set-ups by ensemble averaged spectra and cospectra of water vapour fluxes and compared them with temperature spectra and cospectra.

Additionally, we followed the Kolmogorov law (Kolmogorov, 1991), which describes a theoretical energy decrease with increasing frequency in the inertial sub-range of $-5/3$. The same theory formulates an energy decrease of $-2/3$ for scalars and $-4/3$ for covariances in the inertial sub-range (Foken et al., 2004), if multiplied by the frequency. The inertial sub-range is the region of the spectrum where neither dissipation nor the generation of turbulent kinetic energy is important for the respective eddy. The eddies in the inertial sub-range receive energy from larger eddies and pass it on to smaller eddies (Stull, 1989). The corresponding results are presented in Sect. 3.5.

The spectral response characteristics of the LI-7200 gas analyser and the low-cost thermohygrometer were further investigated in terms of the cut-off frequency, f_c, derived from true water vapour spectra. We estimated the cut-off frequency as the frequency of the intercept between the maximum water vapour spectral energy and the linear fit of the energy spectrum in the inertial sub-range (between 0.1 and 1 Hz) on a double logarithmic scale (see Fig. 3 for clarification). From the cut-off frequency we estimated the sensors time constant, τ_c, with the following relationship

$$\tau_c = 1/(2\pi f_c) \qquad (13)$$

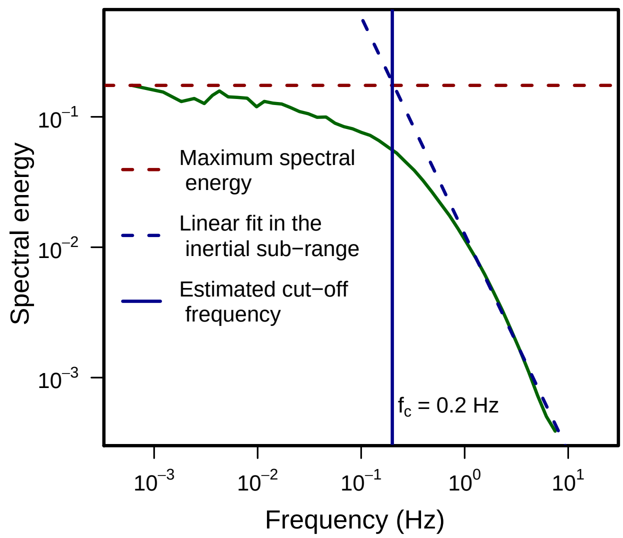

Figure 3. Sketch of the cut-off frequency estimation procedure with an exemplary true water vapour spectrum against frequency.

3 Results and discussion

3.1 Meteorological conditions

The measuring period at the monocultural agriculture plot of Dornburg (16-June to 14-July 2016) was characterized by high air temperature with a maximum daily mean of 25 °C and an average over the whole period of 18 °C (Fig. 4 (a) and Table A1). Cumulative precipitation over the period was low, with only 2 mm (Fig. 4 (a)). The low amount of rainfall caused a rapid ripening of the crops, which had a significant impact on the turbulent fluxes: evapotranspiration decreased and the sensible heat fluxes increased during the measuring period of four weeks.

In contrast, the measuring period (14-July to 12-August 2016) at the agroforestry plot in Dornburg (Fig. 4 (b)), about 500 m apart from the monocultural plot, was characterized by warm (mean air temperature of 19 °C) and humid ambient conditions with a cumulative precipitation of about 50 mm and a mean vapour pressure deficit (VPD) of 6.41 hPa. At the time of installation of the EC set-up the crops were already mature whilst the trees were at the seasonal maximum of their productivity.

The weather conditions during the measuring period at the agroforestry plot in Reiffenhausen (12-August to 14-September 2016, Fig. 4 (c)) were warm with mean daily air temperatures above 15 °C and a total mean of 19.31 °C. The period was characterized by a few intense precipitation events with a cumulative sum of 26.3 mm (Table A1) and a mean VPD of 8.02 hPa.

The following measuring campaign in Wendhausen (03-May to 02-June 2017) was characterized by low mean VPD values of 5.4 hPa at the agforestry plot and 5.2 hPa at the ~~agforestry and monocultural plot, respectively~~monoculural plot. At the beginning of the campaign, mean air temperature was at its lowest between 10 °C and 15 °C, whilst at the end air temperature was between 15 °C and 20 °C~~(~~. The mean air temperature was 16.6 °C at the agforestry plot and 15.5 °C at the ~~agforestry and monocultural plot , respectively,~~ monoculural plot (Fig. 4 (d) and Table A1). Plants were very productive in terms of transpiration both at the agroforestry (trees and crops) and the monocultural (only crops) plots.

In contrast, the campaign period in Forst (08-June to 08-July 2017) was very warm ~~(~~with mean air temperature of 21.4 °C at the agroforestry plot and 21.2 °C ~~, agroforestry and monocultural plot, respectively) and dry with low cumulative precipitation and high~~ at the monocular plot. High VPD values of around 12 hPa indicate dry ambient conditions.

3.2 Evapotranspiration rates from conventional- and low-cost eddy covariance

Diel cycles of evapotranspiration were well represented by the EC-LC set-up compared to the EC set-up on a 30-minute time scale (Fig. 5) at all sites. On a longer time scale (over a period of four weeks) the EC-LC set-up showed changes in daily summed evapotranspiration rates from higher sums ($\approx$ 6 $\mathrm{mm\,d^{-1}}$) at the beginning and lower sums ($\approx$ 3 $\mathrm{mm\,d^{-1}}$) at the end of the measuring period (from 16-June to 14-July 2016~~, Fig. 5 (f)~~) at the monocultural agriculture plot of Dornburg in the same way as the EC set-up did (Fig. 5 (f)). We interpret this as a result of the ripening process of the crops. The ripening process was intensified by an exceptionally low cumulative precipitation of about 2 mm over the entire campaign period (Fig. 4 (a)) and a resulting low soil water content (not shown).

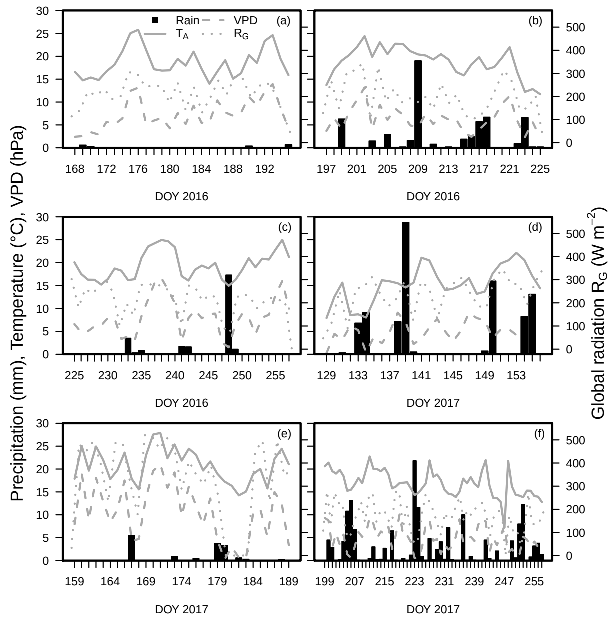

Figure 4. Daily averaged air temperature, vapour pressure deficit (VPD), daily summed precipitation and averaged global radiation, R_G, for the following plots at each subfigure: Dornburg monoculture, (a), Dornburg agroforestry, (b), Reiffenhausen agroforestry, (c), Wendhausen, (d), Forst, (e) and Mariensee, (f). For Wendhausen, Forst and Mariensee, we took the average between the agroforestry and monocultural plot to provide a general overview of the meteorological conditions during the campaign. The averaging was done because both plots at the three sites were sampled simultaneously and the distance between both plots was maximum 600 m. We assumed similar weather conditions.

3.3 Effect of spectral- and WPL corrections on evapotranspiration rates from low-cost eddy covariance

A linear regression analysis between the uncorrected and the fully corrected evapotranspiration rates yielded a slope of 0.74 (R^2 = 99 %) (Fig. 6). The applied corrections accounted for an increase of 26 % of the overall flux magnitude.

The low-frequency cospectral correction after Moncrieff et al. (2004) accounted for 1 % of the fully corrected flux, which was the smallest contribution of all corrections to a flux magnitude increase.

The WPL correction yielded an increase of the flux magnitude of about 2 %. Other studies found an increase in the mean latent heat flux of 5.6 % (Mauder and Foken, 2006) when the WPL correction was applied. In the study of Mauder and Foken (2006), the WPL corrected latent heat flux measured with a LI-7500 open-path EC system was compared with an uncorrected flux from the same EC complex.

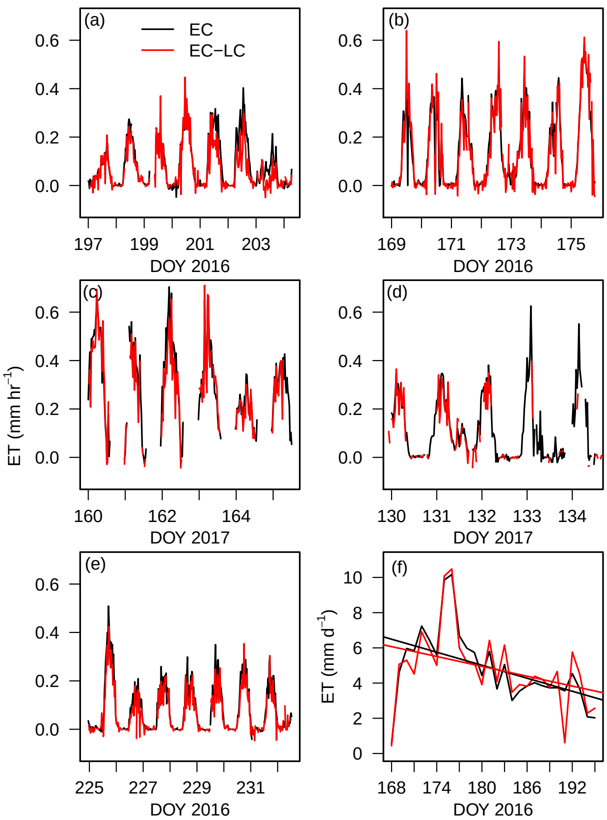

Figure 5. Half hourly evapotranspiration rates of one exemplary week, measured with the conventional EC- (black) and the EC-LC set-up (red) for Dornburg agroforestry, (a), Dornburg monoculture, (b), Forst agroforestry, (c), Wendhausen agroforestry, (d), Reiffenhausen agroforestry, (e). Subfigure (f) shows time series of daily summed evapotranspiration for the EC and EC-LC set-ups for Dornburg monoculture over the whole campaign period (from 16-June to 14-July 2016). ~~The~~ We included the linear trend lines ~~for the EC and EC-LC set-ups~~ with a slope of -0.1232 $\mathrm{mm\,d^{-1}}$ ~~with~~ and a p-value of 0.009595 (black line) for the EC set-up and a slope of -0.09337 $\mathrm{mm\,d^{-1}}$ ~~and~~ with a p-value of 0.06549 (red line) ~~, respectively, are shown~~for the EC-LC set-up.

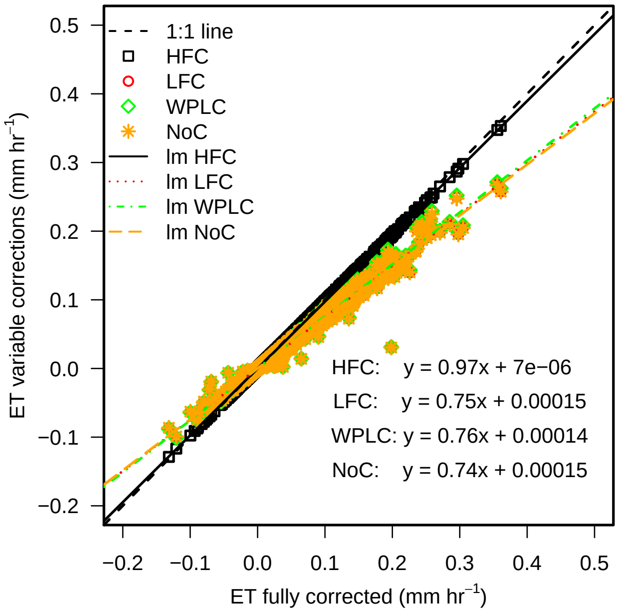

Figure 6. Evapotranspiration rates with the following corrections applied separately: 1) the high-frequency cospectral correction after Moncrieff et al. (1997) (HFC, black squares), 2) the low-frequency cospectral correction after Moncrieff et al. (2004) (LFC, red circles), 3) WPL correction after Webb et al. (1980) (WPLC, green diamonds) and 4) no correction (NoC, yellow stars) versus the fully corrected evapotranspiration rates of the EC-LC data set from Dornburg agroforestry. The best fit line with the same colours as the corresponding data points and the linear regression results for the respective corrections are shown. The linear regression is based on 1381 data points gathered during the campaign from the 14-July to 12-August 2016.

The high-frequency correction after Moncrieff et al. (1997) accounted for 23 % of the fully corrected flux, which was the largest contribution of all corrections to a flux magnitude increase. We interpret the high contribution of the correction from Moncrieff et al. (1997) as a result of the low response time of the thermohygrometer. In ~~a study by Ibrom et al. (2007) ,~~ Ibrom et al. (2007) the low-pass filtering properties of the closed-path system led to an underestimation of the measured latent heat flux and resulted in a necessary correction of 42 %.

The overall impact of spectral corrections on a change of the turbulent latent heat fluxes was stronger for the EC-LC set-up compared to the EC set-up. Here, we quantify the overall impact of spectral corrections on latent heat fluxes in terms of the spectral correction factor (SCF) calculated for each 30-minute period. The 30-minute SCF was multiplied with the respective uncorrected flux. A SCF larger than one indicates a flux magnitude increase, whereas a SCF lower than one indicates a flux magnitude decrease. Box-whisker plots of 30-minute SCFs for each site and each set-up are shown in Figure 7 (a). We found a mean SCF of 1.96 ± 0.64

for the EC-LC set-up and 1.14 ± 0.05 for the EC set-up across all sites, indicating a mean flux magnitude increase of 96 % for the EC-LC set-up and a mean flux magnitude increase of 14 % for the EC set-up. The mean SCF presented here integrates both night and day time periods. Thus, a high SCF during night time with commonly low latent heat fluxes leads to a smaller change of the flux magnitude than during day time, when fluxes are commonly high. Therefore, we also present the sum of 30-minute ET rates corrected for spectral losses and the sum of the total ET attributed to the spectral corrections in Figure 7 (b). The part of the total corrected ET attributed to the spectral corrections was higher for the EC-LC set-up compared to the EC-set-up and amounted on average to 42.7 ± 14.1 % of total ET for the EC-LC set-up and 9.3 ± 3.3 % of total ET for the EC set-up.

Across sites, we found the highest median spectral correction factor of 3.01 and the highest part of the total corrected ET attributed to the spectral corrections of 60.9 % for the EC-LC set-up at the monocultural agriculture plot of Dornburg. We interpret this as a measurement height dependency of the spectral corrections. The measurement height at the agroforestry plots was 10 m and at the monocultural agriculture plots the measurement height was 3.5 m. We assume that high-frequency eddies are more likely close to the surface. Therefore, a detected turbulent signal at the lower measurement height would be shifted towards high frequencies compared to the detected turbulent signal at the higher measurement height (Aubinet et al., 2012). If a sensor is not capable of detecting the turbulent signal in the high frequency range of the spectrum, the signal is attenuated and needs to be corrected.

3.4 Sensor cut-off frequency and time constant

The nominal time response of the relative humidity sensor as part of the thermohygrometer yields a theoretical sensor cut-off frequency of 0.16 Hz (6.3 s) calculated from Eq. 13.

Under field conditions we observed a mean cut-off frequency of 0.063 ± 0.02 Hz for the low-cost thermohygrometer and 0.3 ± 0.2 Hz for the LI-7200 gas analyser across five plots and all humidity classes (from 30 % to 90 % relative humidity bins). The respective mean time constant was 2.8 ± 1 s for the low-cost thermohygrometer and 0.6 ± 0.3 s for the LI-7200 gas analyser (see Fig. 8). For both sensors we found an exponential increase of the time constant with relative humidity (see Fig. 8).

Under field conditions, the cut-off frequency and the respective time constant of the thermohygrometer were inferior to the one given in the specifications. We interpret this as caused by the design of the enclosure. The thermohygrometer is placed at the end of a cylinder with the ventilator directly below, so that the flow velocity is decelerated. Subsequently, the decelerated flow velocity leads to a limited signal response. One suggestion for improvement of the frequency response would be to place the thermohygrometer inside a longer tube with a freely moving air stream. This ensures a faster air exchange inside the measurement cell of the thermohygrometer and hence a faster response time.

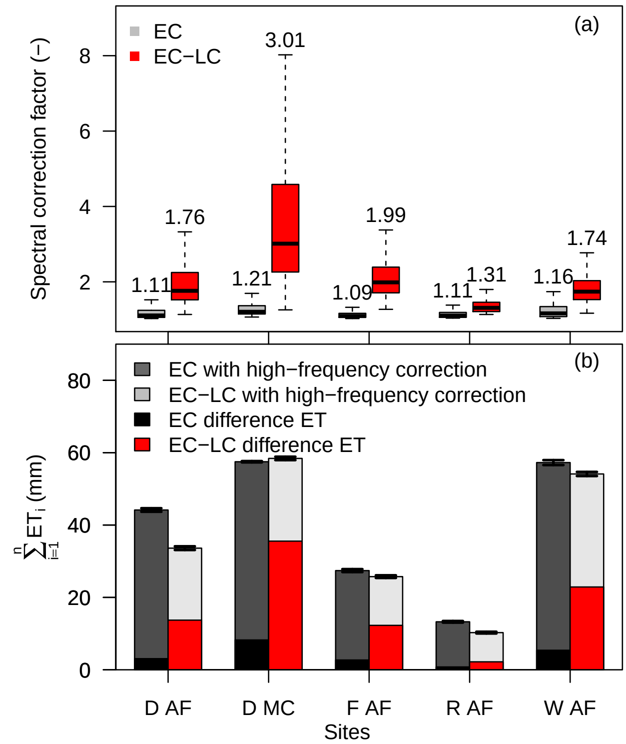

Figure 7. a) Box-whisker plot of spectral correction factors for the EC (grey) and the EC-LC (red) set-up for all sites. Values above the bars correspond to the median spectral correction factor, and, b) cumulative evapotranspiration rates for the EC and EC-LC set-ups for all sites, e.g Dornburg agroforestry, (D AF), Dornburg monoculture, (D MC), Forst agroforestry, (F AF), Wendhausen agroforestry, (W AF), and Reiffenhausen agroforestry, (R AF), over the respective campaign periods (Table A2). The error bars in Figure (b) correspond to the summed random uncertainties. The black and red bars correspond to that part of the total ET attributed to the high-frequency correction for the EC and EC-LC set-up, respectively. Incomplete records with either of EC or EC-LC missing were omitted.

3.5 Spectral analysis

3.5.1 Ensemble averaged spectra of the water vapour mole fraction and sonic temperature and their dependency on relative humidity

The match of the water vapour mole fraction spectra with the theoretical -2/3 slope was found to be dependent on relative humidity. We observed the least deviation of the water vapour spectra obtained by the EC and EC-LC set-ups from the theoretical -2/3 slope for low relative humidity (Fig. 9). The relative humidity dependency of the water vapour spectra is a

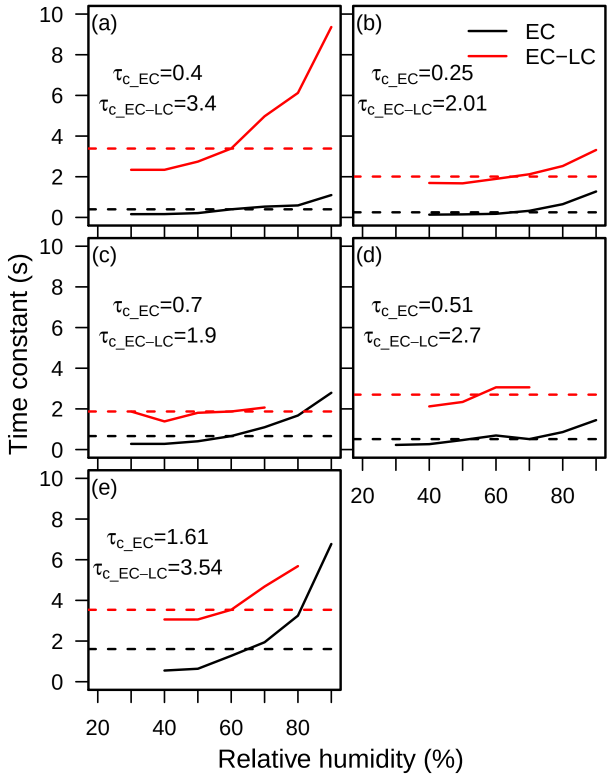

Figure 8. Time constant against relative humidity for the LI-7200 (black solid lines) and the thermohygrometer (red solid lines). Dashed lines with the same colour coding as for data shown and values written, correspond to the mean time constant for the respective sensors across all relative humidity classes. Sites correspond to Dornburg agroforestry, (a), Dornburg monoculture, (b), Forst agroforestry, (c), Reiffenhausen agroforestry, (d), and Wendhausen agroforestry, (e).

known feature for closed- and enclosed-path gas analysers. Fratini et al. (2012) reported the same behaviour for both short (4 m) and very short (1 m) sampling lines. The so called "amplitude attenuation effect" (Fratini et al., 2012) was explained by Ibrom et al. (2007) as a result of absorption and desorption of water vapour molecules by hygroscopic particles inside the tube. Absorption and desorption processes are more pronounced at higher relative humidity and follow an exponential dependency on increasing relative humidity (Fratini et al. (2012), Ibrom et al. (2007)).

The spectral response characteristics of the ~~conventional~~ EC set-up were superior to the ones from the EC-LC set-up. The water vapour spectra from the EC-LC set-up deviated more from the theoretical -2/3 slope than the EC set-up in the inertial sub-range (between 0.1 Hz and 1 Hz) (Fig. 9). The ultrasonic temperature spectra followed a slope of -2/3 in the particular range of the energy spectrum, as the measurements are open-path.

For frequencies higher than 1 Hz, an increase of the spectral energy of water vapour for two out of five plots and both set-ups (i.e. Forst and Wendhausen agroforestry, Fig. 9 (c) and (d)) was observed, whereas the water vapour spectral energy increase for the agroforestry and monocultural plots of Dornburg and Reiffenhausen agroforestry was only found for the EC-LC set-up. We interpret the spectral energy increase of water vapour in the particular frequency range as sensor noise, as indicated by the f^1 slope for white noise (Eugster and Plüss, 2010) in Fig. 9. The ultrasonic temperature spectra showed a slight spectral energy increase from frequencies higher than 4 to 5 Hz, which we interpret as an attenuation effect caused by the path-averaging (Kristensen and Fritzjarrals, 1984).

The observed noise of the water vapour spectra obtained by the EC set-up at the agroforestry plots of Forst and Wendhausen (Fig. 9 (c) and (d)) might be caused by different tube diameters in 2016 and 2017. In 2017 a thicker tube with an inner diameter of 8.2 mm was used compared to 2016 (inner tube diameter of 5.3 mm). In both years, a flow rate of 15 slpm was applied. The change in the inner tube diameter led to more turbulent conditions within the thinner tube than within the thicker tube. The thinner tube had a Reynolds number of 3950.6 (towards turbulent flow) and the thicker tube had a Reynolds number of 2551.71 (towards laminar flow).

3.5.2 Ensemble averaged cospectra of the water vapour flux and sensible heat flux

The water vapour flux cospectra deviated negatively from the theoretical -4/3 slope for the EC and EC-LC set-ups between a normalized frequency of 0.1 and 8 (the inertial sub-range) for all sites (Fig. 10). The deviation from the -4/3 slope in this particular frequency range was strongest for the EC-LC set-up, which is result of the limited spectral response characteristics of the thermohygrometer. ~~The~~ As discussed in Section 3.4 the response time of ~~1 second for a relative humidity change from 0 % to 90 % and vice versa automatically filters eddies of frequencies higher than 1 Hz~~the thermohygrometer was lower than given in the specifications.

The water vapour flux cospectra of the conventional EC set-up at the agroforestry plots of Forst and Wendhausen (Fig. 10 c) and d)) showed a stronger attenuation in the inertial sub-range, compared to the agroforestry plot and the monocultural agriculture plot of Dornburg and the agroforestry plot of Reiffenhausen (Fig. 10 a), b) and e)). That was likely caused by the different tube diameter at the respective plots and the effect on the turbulence characteristics inside the tubes, as discussed in Sect. 3.5.1.

At normalized frequencies higher than 8, we found a slope decrease of the water vapour flux cospectra obtained by the EC-LC set-up at all sites, which we interpret as an effect of sensor noise. Assuming that the vertical wind velocity measurements are unaffected by sensor noise, only the thermohygrometer measurements contribute to the slope decrease

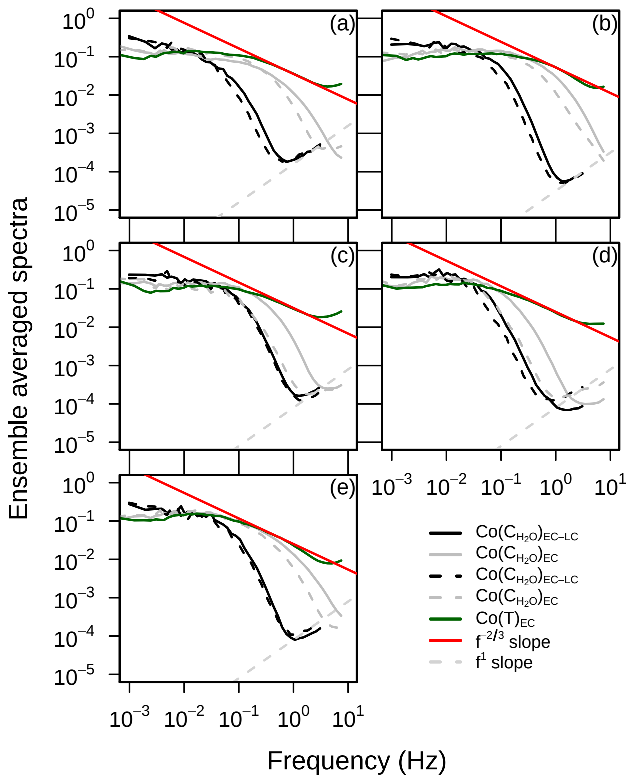

Figure 9. Ensemble averaged normalised water vapour and temperature spectra for relative humidity thresholds of 60 % (solid lines) and 80 % (dashed lines) versus the natural frequency. Spectra of the EC set-up (grey) and the EC-LC set-up (black) are shown. Subfigures correspond to plots: Dornburg agroforestry, (a), Dornburg monoculture, (b), Forst agroforestry, (c), Wendhausen agroforestry, (d), and Reiffenhausen agroforestry, (e). Spectra were filtered for low quality data, corresponding to a flag of 2 following the procedure of Mauder and Foken (2011a) and according to spike removal methods described in Vickers and Mahrt (1997). Relative humidity classes correspond to ancillary relative humidity measurements.

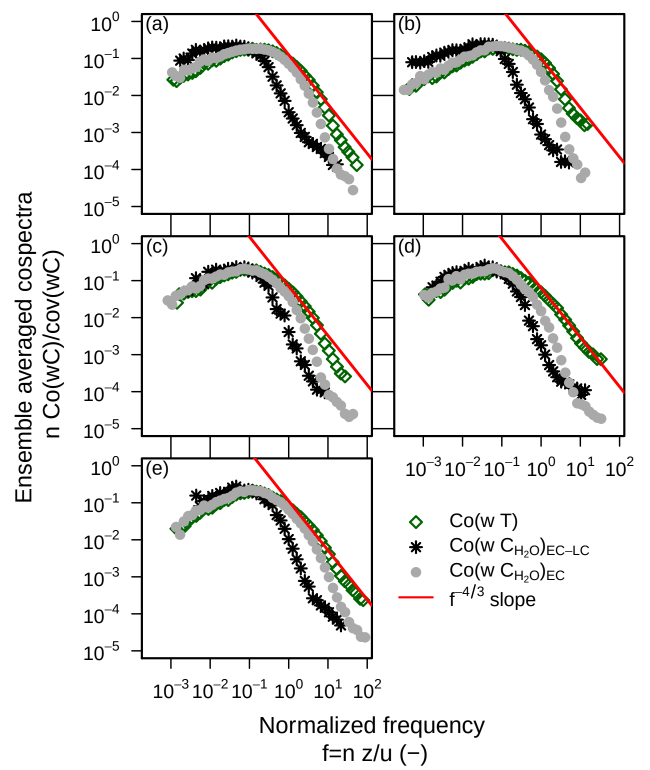

Figure 10. Ensemble averaged ~~evapotranspiration~~ cospectra of the water vapour flux for the EC- and the EC-LC ~~set-up~~ set-ups (grey and black dots, resp.) and the ~~temperature~~ cospectrum of the sensible heat flux (green dots) versus the normalized frequency over the entire campaign period for Dornburg agroforestry, (a), Dornburg monoculture, (b), Forst agroforestry, (c), Wendhausen agroforestry, (d), and Reiffenhausen agroforestry, (e). Cospectra shown correspond to an unstable stratified atmosphere according to a Monin-Obukhov length between $-650 < L < 0$. Cospectra were filtered for low quality data, corresponding to a flag of 2 following the procedure of Mauder and Foken (2011a) and according to spike removal methods described in Vickers and Mahrt (1997).

of the water vapour flux cospectra found in Fig. 10 for the EC-LC set-up.

In the low-frequency range (for a normalized frequency < 0.1) of the turbulent spectrum, the normalized water vapour cospectrum obtained by the EC-LC set-up was higher than the temperature cospectrum (Fig. 10). We interpret this finding as an effect of aliasing, which is an increased spectral energy in the low-frequency range due to a wrong representation of the high frequencies (Foken, 2008). That implies a too high sampling frequency relative to the sensors response time. The effect of aliasing was also observed for the EC cospectrum, but was much lower compared to the EC-LC set-up.

3.6 Water vapour molar densities from the thermohygrometer and the LI-7200 gas analyser

The water vapour molar density calculated from the thermohygrometer output showed to be a smoothed version of the water vapour molar density directly measured by the LI-7200 gas analyser, as shown for a time period of one hour for the agroforestry plot of Dornburg in Fig. 11. The low-frequency fluctuations were captured, whereas the high-frequency fluctuations were attenuated. A linear regression analysis between both water vapour molar densities yielded a R^2 value of 0.85 (based on 29419 data points). We interpret the smoothed water vapour molar density calculated by the thermohygrometer set-up as an effect of the longer response time of the thermohygrometer and the limited sampling frequency of 8 Hz. Spectral analysis of the water vapour mole fraction (Sections 3.5.1 and Fig. 9) derived from the thermohygrometer confirmed the attenuation of high frequencies by the thermohygrometer. The water vapour spectra from the thermohygrometer showed a strong deviation from the theoretical -2/3 slope and from the temperature spectrum at frequencies higher than 0.1 Hz. For frequencies lower than 0.1 Hz the water vapour spectra compared well with the temperature spectrum.

The molar density derived from the thermohygrometer was on average about 100 $\mathrm{mmol\,m^{-3}}$ higher than the molar density measured by the LI-7200 gas analyser during the one hour period. A mean value of 606.32 $\mathrm{mmol\,m^{-3}}$ was found for the thermohygrometer and 514.8 $\mathrm{mmol\,m^{-3}}$ for the LI-7200 gas analyser. We interpret the higher water vapour density derived from temperature, relative humidity and air pressure measurements from the thermohygrometer as an effect of the temperature measurements from the thermohygrometer. We found a 5 °C higher air temperature from the thermohygrometer compared to the sonic temperature under clear sky condition~~(Fig. ?? for an exemplary day)~~. The temperature difference is caused by a radiation effect originating from the PVC housing.

In addition, the temperature measurements from the thermohygrometer were attenuated compared to the sonic temperature~~(Fig. ??)~~. We interpret this as an inertia effect of the thermohygrometer. So, if the thermohygrometer complex has a higher thermal mass than the ambient air, the temperature measurements taken by the thermohygrometer are attenuated in the high-frequency range. As the attenuation effect was not found in the relative humidity measurements, we assume that the relative humidity measurements were independent of temperature measurements and therefore relative humidity was not attenuated in the same way as air temperature. Subsequently, relative humidity fluctuations were conserved and could be used for the calculations of the water vapour mole fraction. ~~For the EC method~~In general, the deviation from the mean is of higher interest than the mean itself for the EC method (Baldocchi, 2014). As long as the relative humidity fluctuations are conserved in the calculations of the water vapour mole fraction, a plausible covariance between the water vapour mole fraction and the vertical velocity can be calculated.

3.7 Linear regressions of ~~ET rates~~ latent heat fluxes from conventional- and low-cost eddy covariance

Results of a linear regression analysis between evapotranspiration rates obtained by the EC and EC-LC set-ups revealed a dependency of the evapotranspiration rates on the high-frequency cospectral correction method used. Evapotranspiration rates obtained by the EC-LC set-up using the Ibrom et al. (2007) high-frequency cospectral correction underestimated evapotranspiration rates obtained by EC using the high-frequency correction after Ibrom et al. (2007) (always used for the EC set-up) at all sites (Table 2). The largest underestimation was 32 % (Forst agroforestry) and the smallest

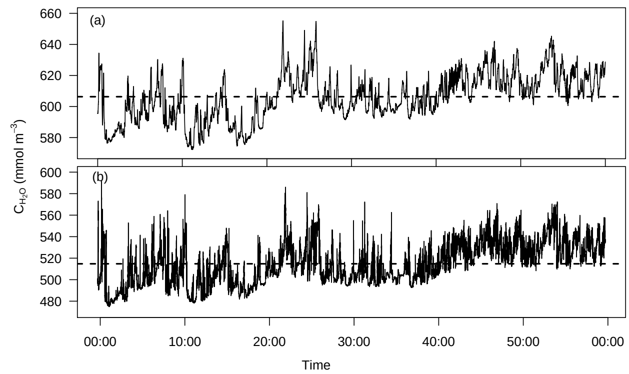

Figure 11. Water vapour molar density time series (solid line) and mean (dashed line) for the thermohygrometer, (a), and the LI-7200 gas analyser, (b), at the Dornburg agroforestry plot. The time series represent a 1-hour period from 14:00 to 15:00 hours on 19-July 2016.

underestimation was 13 % (Dornburg agroforestry), with a median underestimation of 22 % across all five plots.

In contrast, evapotranspiration estimates obtained by the EC-LC set-up using the Moncrieff et al. (1997) high-frequency cospectral correction revealed an underestimation of evapotranspiration rates by the EC-LC set-up of 14 %, 6 %, 5 % and 1 % for the agroforestry plots of Reiffenhausen, Dornburg, Forst and Wendhausen, respectively, and an overestimation by the EC-LC set-up of 8 % for the monocultural agriculture plot of Dornburg ~~compared to conventional EC~~ relative to the conventional EC set-up (Table 2 and Fig. 12).

The dependency of the evapotranspiration estimates on the chosen high-frequency cospectral correction method may be caused by the assumptions of each method. The Ibrom et al. (2007) high-frequency correction method was initially developed for a closed-path eddy covariance system, with a tube length of about 50 m. The method described in Ibrom et al. (2007) takes into account the dependency of water vapour concentration measurements on relative humidity effects inside the tube. ~~Therefore, independent meteorological measurements of relative humidity and air temperature were required, when the method after Ibrom et al. (2007) was applied.~~ A low-pass cut-off frequency was estimated for each 30-minute period as a function of ambient relative humidity. At least one month of data are suggested to estimate the low-pass cut-off frequency (LI-COR, 2015).

~~The~~ In contrast, the high-frequency correction method after Moncrieff et al. (1997) is purely analytical and applies a fit of the temperature cospectra measured with the sonic anemometer on the water vapour cospectra. This analytical method can be applied independently of meteorological measurements. Furthermore, the correction after Moncrieff et al. (1997) was recommended for either open-path EC systems or under conditions when the intake tube is short and heated (LI-COR, 2015).

From an analysis of the high-frequency transfer function from Moncrieff et al. (1997) and the Lorentzian of the infinite impulse response filter from Ibrom et al. (2007) it is evident that the correction of high-frequency losses is better represented by the high-frequency spectral correction of Moncrieff et al. (1997) (see Fig. 13). The transfer function after Moncrieff et al. (1997) is shifted towards higher frequencies and lower frequencies are conserved. According to the Lorentzian (Ibrom et al., 2007) the filtering properties are more pronounced for Ibrom et al. (2007) and low-frequencies ($<10^{-2}$ Hz) are attenuated. Based on the assumptions and recommendations given in Moncrieff et al. (1997) and LI-COR (2015), we decided to apply the correction of Moncrieff et al. (1997) to our EC-LC set-up.

Currently, the authors of the only known study published by Hill et al. (2017) presents a low-cost EC set-up for measurements of CO_2 and water vapour fluxes. The authors compared the low-cost EC set-up with a LI-7500 gas analyser sharing the same Campbell Scientific CSAT3 sonic anemometer. They reported a 6 % flux magnitude overestimation of the latent heat flux obtained by the low-cost EC system relative to the reference EC set-up.

Flux magnitude differences observed for our low-cost set-up are comparable to flux magnitude differences between conventional EC set-ups observed in a recently published study by Polonik et al. (2019). The authors found average differences between 4 % and 14 % between water vapour fluxes obtained by different EC set-ups consisting of three different sonic anemometers and five conventional gas analysers.

3.8 Dependency of the latent heat flux random uncertainty on relative humidity

Common to all sites and both set-ups was a decreasing absolute random uncertainty of the latent heat flux with increasing relative humidity (Fig. 14). At high relative humidity turbulent latent heat fluxes were low, commonly during night time and bad weather conditions. Whereas, during day time and good weather conditions (generally low relative humidity), the fluxes were high. Richardson et al. (2006) described a linear dependency of the absolute random uncertainty on the magnitude of the turbulent fluxes.

For three out of five plots (Dornburg agroforestry and monoculture and Reiffenhausen agroforestry, respectively, Fig. 14 (a), (b) and (e)), we found a lower median random uncertainty for the latent heat fluxes obtained by the conventional EC set-up at low relative humidity, compared to the EC-LC set-up. At high relative humidity (≥ 70 %) the median of both random uncertainties was equal.

For the other two plots (Fig. 14 (c) and (d)) either a higher or nearly equal mean and standard deviation was found for the latent heat flux random uncertainty from the EC set-up compared to the EC-LC set-up. Furthermore, the standard deviation of the random uncertainty of the latent heat fluxes

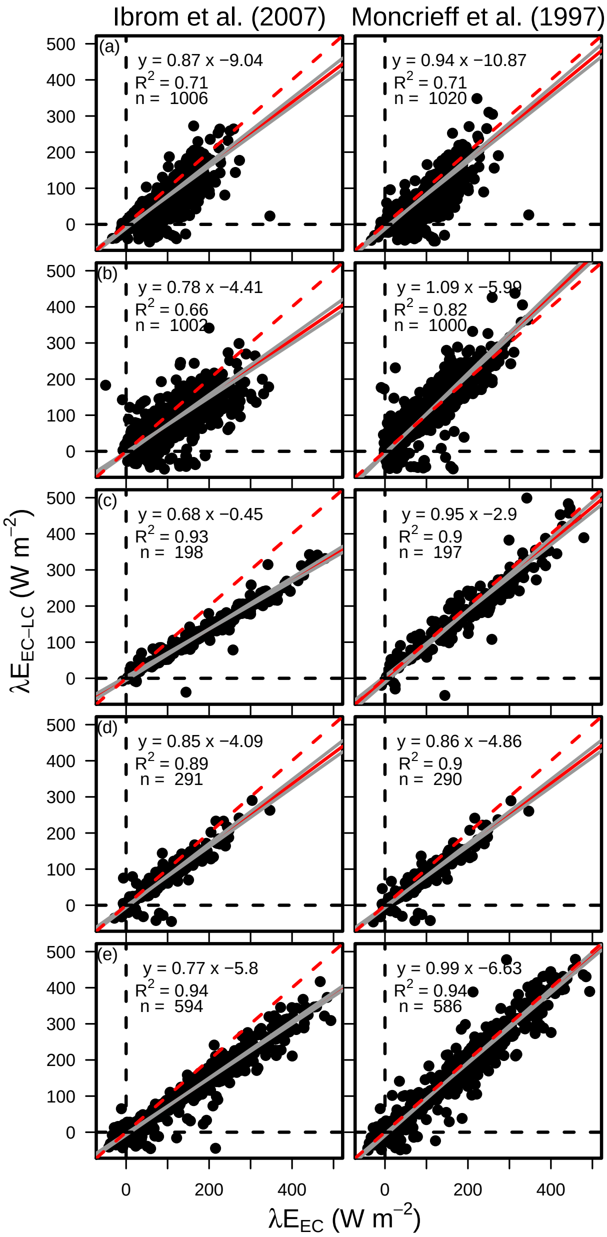

Figure 12. Scatter plots of latent heat fluxes obtained by the low-cost EC set-up versus latent heat fluxes obtained by the conventional EC set-up for Dornburg agroforestry, (a), Dornburg monoculture, (b), Forst agroforestry, (c), Reiffenhausen agroforestry, (d), and Wendhausen agroforestry, (e). Latent heat fluxes obtained by the conventional EC set-up were corrected for high-frequency losses by the high-frequency correction method of Ibrom et al. (2007), whereas the latent heat fluxes obtained by the low-cost EC set-up were corrected by, first, the high-frequency correction method of Ibrom et al. (2007) (left site) and, second, the high-frequency correction method of Moncrieff et al. (1997) (right hand site).

Table 2. Major axis linear regression of evapotranspiration from EC-LC versus EC, using two high-frequency correction methods (Ibrom et al. (2007) and Moncrieff et al. (1997)). The slopes include the $\pm 2.5\,\%$ confidence interval. The root mean square error, RMSE, and the coefficient of determination, R^2, are given.

Correction method	Ibrom et al. (2007)			Moncrieff et al. (1997)		
Site	Slope/ Intercept	R^2	RMSE ($W\,m^{-2}$)	Slope/ Intercept	R^2	RMSE ($W\,m^{-2}$)
Dornburg AF	0.87±0.034/ -9.04	0.71	36.0	0.94±0.036/ -10.87	0.71	35.13
Dornburg MC	0.78±0.030/ -4.3	0.71	50.8	1.08±0.027/ -5.12	0.86	34.31
Forst AF	0.68±0.026/ -0.45	0.93	74.9	0.95±0.045/ -2.9	0.90	38.5
Wendhausen AF	0.78±0.016/ -5.8	0.93	53.71	0.99±0.021/ -6.63	0.94	33.5
Reiffenhausen AF	0.85±0.034/ -4.1	0.90	28.13	0.86±0.032/ -4.86	0.90	29.7

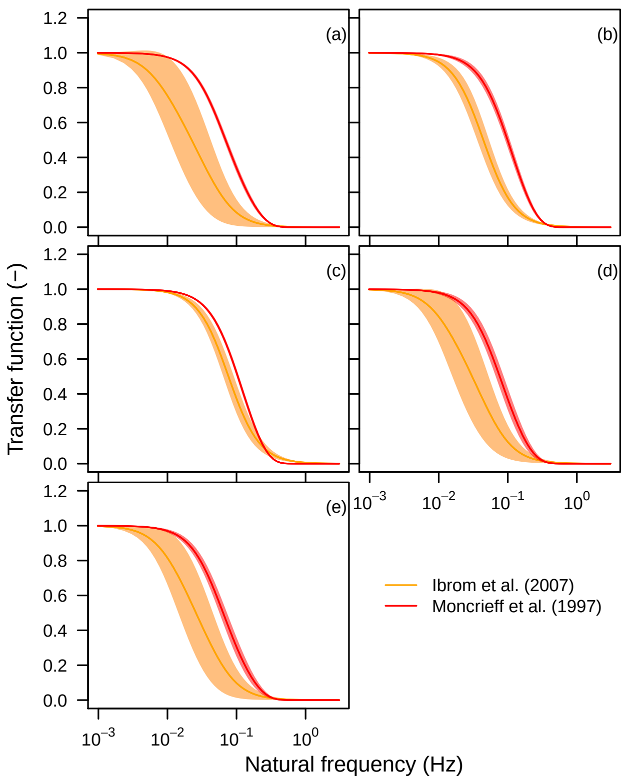

Figure 13. Mean and standard deviation of the spectral correction transfer functions vs. the natural frequency for the high-frequency spectral correction methods of Ibrom et al. (2007) and Moncrieff et al. (1997), respectively, for sites, e.g. Dornburg agroforestry, (a), Dornburg monoculture, (b), Forst agroforestry, (c), Reiffenhausen agroforestry, (d), and Wendhausen agroforestry, (e). The transfer function after Ibrom et al. (2007) represent the mean over all infinite impulse response (IIR) filters, approximated by the Lorentzian $H_{IIR}(f|f_c) = \frac{1}{1+(f/f_c)^2}$. $H_{IIR}(f|f_c)$ was estimated for each 30-min period as per the mean ambient relative humidity.

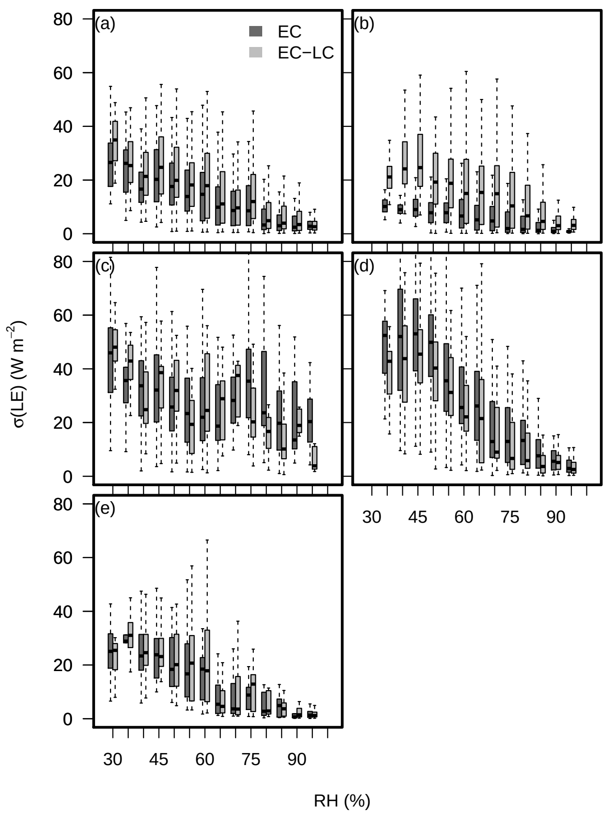

Figure 14. Box-whisker plots with random error uncertainty of the latent heat flux calculated by the EC and EC-LC set-up, respectively, versus relative humidity bins of 5 %. Subfigures correspond to plots: Dornburg agroforestry, (a), Dornburg monoculture, (b), Forst agroforestry, (c), Wendhausen agroforestry, (d), and Reiffenhausen agroforestry, (e).

obtained by the EC and EC-LC set-ups was of the same order of magnitude as their respective mean (Table 3).

3.9 Distribution of differences between evapotranspiration estimates

The median of differences between evapotranspiration rates obtained by the EC and EC-LC set-up was negative for the

Table 3. Mean random uncertainties and standard deviations of the latent heat fluxes obtained by the EC and EC-LC set-up.

Site	$\overline{\sigma(LE_{EC})}$	$\overline{\sigma(LE_{EC-LC})}$
Dornburg AF	12.94 ± 15.82	15.76 ± 16.91
Dornburg MC	6.27 ± 6.01	16.23 ± 14.42
Forst AF	30.87 ± 18.84	30.84 ± 18.86
Wendhausen AF	27.45 ± 23.49	23.70 ± 20.93
Reiffenhausen AF	13.2 ± 14.3	14.4 ± 15.7

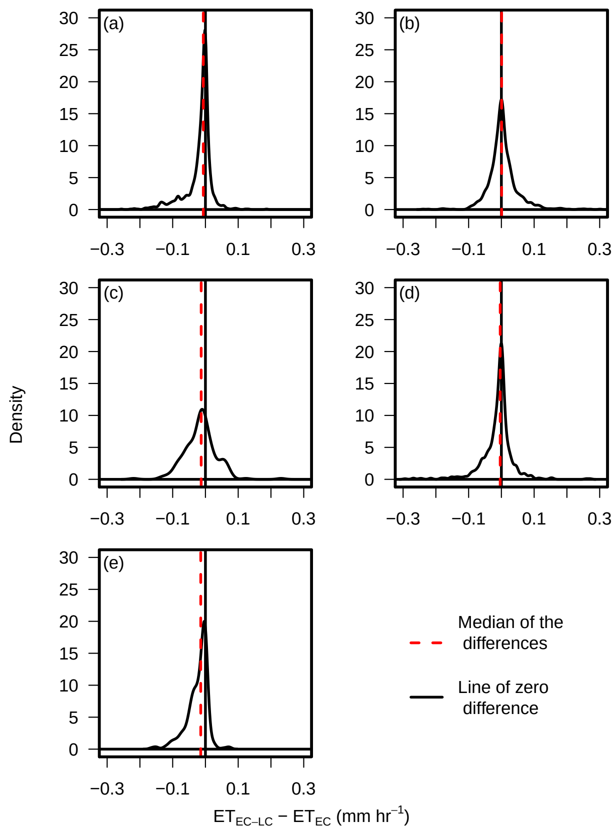

Figure 15. Density distribution of differences between evapotranspiration rates obtained by the EC and EC-LC set-up for Dornburg agroforestry, (a), Dornburg monoculture, (b), Forst agroforestry, (c), Wendhausen agroforestry, (d), and Reiffenhausen agroforestry, (e).

agroforestry plots (Fig. 15 (a), (c), (d) and (e)). This indicates an underestimation of ET rates obtained by the EC-LC set-up, compared to the EC set-up. The distribution of the differences between evapotranspiration rates followed a skewed distribution with a tail towards negative differences of up to ~ -0.15 $\mathrm{mm\,hr^{-1}}$. The tail towards positive values declined sharply after the maximum of the distribution.

At the monocultural agriculture plot at Dornburg (Fig. 15 (b)) there was no significant difference in the median evapotranspiration rates of the two set-ups. The differences were equally distributed towards over- and underestimated ET rates until a zero density of ± 0.1 $\mathrm{mm\,hr^{-1}}$.

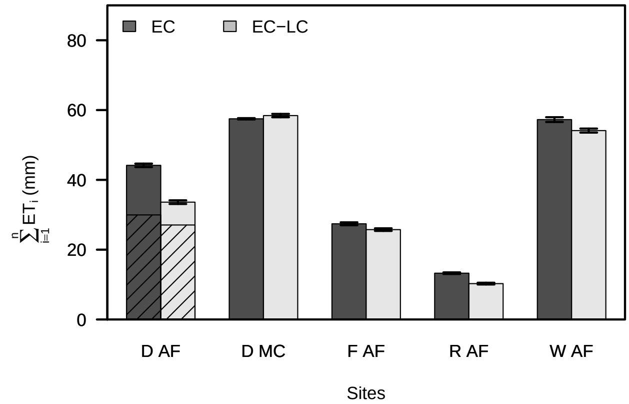

Figure 16. Cumulative evapotranspiration rates for the EC and EC-LC set-ups for Dornburg agroforestry, (D AF), Dornburg monoculture, (D MC), Forst agroforestry, (F AF)~~and~~ , Wendhausen agroforestry, (W AF), and Reiffenhausen agroforestry, (R AF) over the respective campaign periods (Table A2). The error bars correspond to the summed random uncertainties~~, which were added~~. The shaded area at Dornburg agroforestry correspond to the cumulative ~~evapotranspiration rates~~sum of ET filtered for the period of poor performance of the EC-LC set-up. Incomplete records with either of EC or EC-LC missing were omitted.

3.10 Cumulative evapotranspiration rates

We observed a lower cumulative evapotranspiration for the EC-LC set-up at all agroforestry plots, ~~compared~~ relative to the conventional EC set-up (Fig. 16 and 17). In contrast, a higher cumulative ET was found for the EC-LC set-up at the monocultural agriculture plot of Dornburg. The plot of cumulative ET lines in Figure 17 (a I) indicates a discrepancy between the cumulative ET lines at the agroforestry plot of Dornburg. This is caused by a period of poor performance of the low-cost set-up. After removing this period from the data set, we still observed higher ET sums at the AF than at the MC plot, but now differences were comparable to differences observed at the other plots, as indicated by the black and red bars in Figure 16. In general, the observation of underestimated or overestimated (agroforestry vs. monocultural plots) ET rates obtained by the EC-LC ~~compared~~ set-up relative to the EC set-up ~~are~~ is in agreement with the linear regression results presented in Section 3.7.

3.11 Annual cumulative ET rates for the agroforestry and the monocultural plot

We wanted to understand how evapotranspiration of agroforestry and monoculture differed. We deployed the EC-LC set-up as a convenient means to obtain continuous long-term evapotranspiration estimates at 30-minute resolution. Here, we present annual cumulative sums of 30-minute evapotranspiration rates for 2016 from all sites, independently of the measuring campaigns.

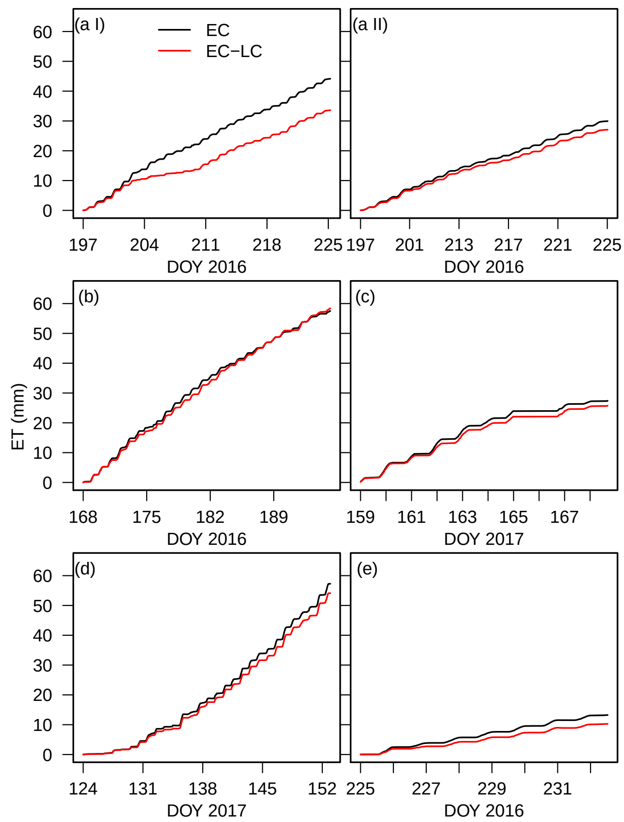

Figure 17. 30-minute cumulative evapotranspiration rates for the EC (solid black line) and EC-LC (solid red line) set-ups for Dornburg agroforestry with unfiltered data for the period of poor performance of the EC-LC set-up, (a I), Dornburg agroforestry with filtered data for the period of poor performance of the EC-LC set-up, (a II), Dornburg monoculture, (b), Forst agroforestry, (c), Wendhausen agroforestry, (d), and Reiffenhausen agroforestry, (e), over the respective campaign periods (Table A2). Incomplete records with either of EC or EC-LC missing were omitted.

At the Dornburg site, annual cumulative evapotranspiration rates were higher at the monocultural agriculture plot compared to the agroforestry plot (Fig. 18), which might be caused by the wind-exposed location of the monocultural agriculture plot. The higher wind speed at the monocultural agriculture plot increases the boundary layer conductance and therefore both soil evaporation and plant transpiration increase.

At the remaining four out of five sites the annual cumulative evapotranspiration rates were higher at the agroforestry plots than at the monocultural agriculture plots (Forst, Wendhausen, Mariensee and Reiffenhausen, Fig. 18). We interpret higher evapotranspiration rates at the agroforestry than at the monocultural plots as an effect of the increased biomass at the agroforestry plot, originating both from the trees and the crops grown between the tree strips. Despite the presence of a leeward side with reduced evapotranspiration caused by the

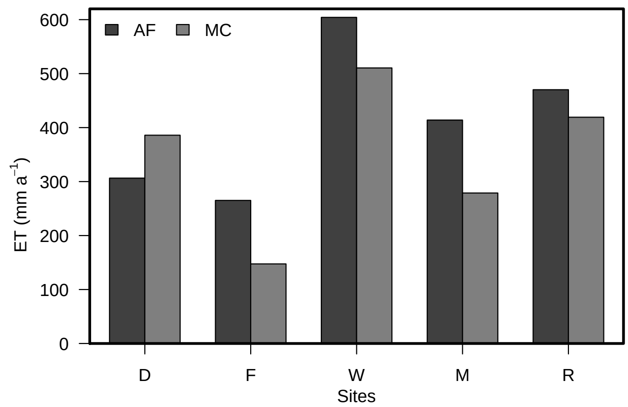

Figure 18. Cumulative evapotranspiration rates obtained by the EC-LC set-up at sites Dornburg, (D), Forst, (F), Wendhausen, (W), Mariensee, (M), and Reiffenhausen, (R), for 2016. Incomplete records with either of agroforestry or monoculture missing were omitted. Gap-filling was performed by multiplying the summed ET with the ratio of the number of maximum possible records to the number of missing records.

wind reduction and the increased shade, both crops and trees are affected by wind on the windward site. More turbulent conditions are present at the agroforestry plots as caused by the presence of the tree strips, which is indicated by a higher mean roughness length at the agroforestry plots compared to the conventional agriculture plots as shown in Fig. A1 for all sites.

4 Conclusions

We presented a new low-cost eddy covariance set-up, which is comprised of a conventional ultrasonic anemometer and a low-cost thermohygrometer. We applied the eddy covariance method on the vertical velocity component and the water vapour mole fraction derived from the thermohygrometer. The advantages of the set-up are low material costs and low power consumption. The performance of the EC-LC ~~method~~ set-up was comparable to the EC ~~method~~ set-up with regards to mean evapotranspiration rates. The ~~method~~ set-up specific differences in mean evapotranspiration rates were insignificant compared to the variability between sites.

In detail, we were able to explain more than 80 % of the variability in evapotranspiration obtained by the conventional eddy covariance set-up by the variability of the low-cost eddy covariance set-up. The low-cost eddy covariance set-up is a good alternative to the conventional EC set-up for both conventional agriculture systems and agroforestry ecosystems at a temporal resolution of 30 minutes.

We showed that under conditions of high relative humidity and low air temperature the flux random error uncertainty of both ~~methods~~ set-ups was highest. ET rates obtained by the EC-LC set-up with limited frequency response had a lower relative difference to ET rates obtained by the EC set-up at the 10 m measurement height (AF) than at the 3.5 m height given a larger contribution of low-frequency eddies at the larger measurement height.

We anticipate potential applications of the EC-LC set-up in experiments comparing different treatments (management effects, different agriculture systems, water use) and chronosequences after fires or clear cuts. The set-up provides a tool for replicated ET measurements across different ecosystems. With low-cost instruments, flux measurements at existing flux networks such as FLUXNET, ICOS or NEON can be complemented and can be provided at remote and so far underrepresented sites.

Data availability. All data used for the figures presented here are provided in the Supplement.

Author contributions. C. Markwitz designed and performed the field work, analyzed the data and has written the current manuscript. Dr. L. Siebicke wrote the project scientific proposal, acquired the funding as part of the BonaRes SIGNAL consortium, and contributed to field work, analysis and manuscript writing.

Competing interests. The authors declare that they have no conflict of interest.

Acknowledgements. We kindly acknowledge the funding from the German Federal Ministry of Education and Research (BMBF, project BonaRes, Modul A: Signal 031A562A) and from the Deutsche Forschungsgemeinschaft (INST 186/1118-1 FUGG). We further wish to acknowledge contributions by A. Knohl and M. Herbst to the BonaRes SIGNAL proposal and project design as well as the technical support of field work received by F. Tiedemann, E. Tunsch, D. Fellert, M. Lindenberg, J. Peters (bioclimatology group) and D. Böttger (soil science group of tropical and subtropical ecosystems) from the University of Göttingen.

Appendix A: ~~Site locations and agroforestry geometry~~

Table A1. Site locations~~and~~, agroforestry geometry and stand characteristics.

Site	Coordinates	No. of tree alleys	System size [m^2]	Relative tree cover	Tree height [m]
Reiffenhausen	51°24'N 9°59'E	3	18700	72%	4.73±0.32 (n=69)
Mariensee	52°34'N 9°28'E	3	69260	6%	4.01±0.33 (n=96)
Wendhausen	52°20'N 10°38'E	6	179738	11.52%	6.21±0.4 (n=114)
Forst	51°47'N 14°38'E	7	391300	12%	6.5±1.8 (n=161)
Dornburg	51°47'N 11°39'E	7	508723	8%	6.4±0.64 (n=160)

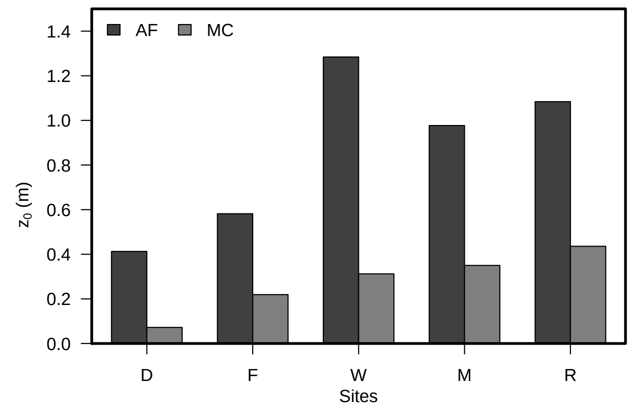

Figure A1. Mean roughness length at sites Dornburg, (D), Forst, (F), Wendhausen, (W), Mariensee, (M), and Reiffenhausen, (R), for 2016.

Appendix B: ~~Time series of relative humidity, air temperature and sonic temperature and meteorological mean variables~~

~~Relative humidity and air temperature measured by the thermohygrometer ((a) and (b), respectively), and the ultrasonic temperature measured by the ultrasonic anemometer, (c), for a 1-hour period on the 19-July, 2016, 14:00 to 15:00 hours at the Dornburg AF plot.~~

Table A2. Temporal extend of the EC measurement campaigns.

Site	Campaign period
Dornburg Conv	16-June to 14-July 2016
Donburg AF	14-July to 12-August 2016
Reiffenhausen AF	12-August to 14-September 2016
Wendhausen	03-May to 02-June 2017
Forst	08-June to 08-July 2017
Mariensee	21-July to 19-September 2017

Table A3. Instrument separation of the gas analyser relative to the centre of the sonic anemometer into the North, East and vertical direction.

Site	North [cm]	East [cm]	Vertical [cm]	Year
Dornburg MC	6	14	-21	2016
Dornburg AF	-27	4	-26	2016
Reiffenhausen AF	1	9	-20	2016
Wendhausen AF	-10	0	-20	2017
Forst AF	-12	0	-22	2017

~~Instrument separation between the sonic anemometer and the gas analyser into the North, East and vertical direction.~~

Table A1. Mean air temperature, T, ~~vapor~~ vapour pressure deficit, VPD, global radiation, R_G and the cumulative precipitation, Rain, for the respective site and measurement period.

Site	T (°C)	VPD (hPa)	R_G (W m^{-2})	Rain (mm)
Dornburg MC	18.6	7.35	212.6	2.1
Dornburg AF	19.0	6.41	200.7	57.1
Reiffenhausen AF	19.31	8.02	219.1	26.3
Wendhausen AF	16.6	5.4	235.0	48.6
Forst AF	21.4	12.02	358.8	18.9

References

Aubinet, M., Vesala, T., and Papale, D., eds.: Eddy Covariance: A Practical Guide to Measurement and Data Analysis, Springer Dordrecht, Heidelberg, London, New York, https://doi.org/10.1007/978-94-007-2351-1, 2012.

Baldocchi, D.: Measuring fluxes of trace gases and energy between ecosystems and the atmosphere - the state and future of the eddy covariance method, Glob. Chang. Biol., 20, 3600–3609, https://doi.org/10.1111/gcb.12649, 2014.

Baldocchi, D. D.: Assessing the eddy covariance technique for evaluating carbon dioxide exchange rates of ecosystems: past, present and future, Glob. Chang. Biol., 9, 479–492, https://doi.org/10.1046/j.1365-2486.2003.00629.x, 2003.

Bosch Sensortec GmbH: BME280: Combined humidity and pressure sensor, 2016.

Bundesamt für Kartographie und Geodäsie: Frankfurt am Main, http://www.bkg.bund.de, 2011.

Burba, G., Schmidt, A., Scott, R. L., Nakai, T., Kathilankal, J., Fratini, G., Hanson, C., Law, B., Mcdermitt, D. K., Eckles, R., Furtaw, M., and Velgersdyk, M.: Calculating {CO_2} and {H_2O} eddy covariance fluxes from an enclosed gas analyzer using an instantaneous mixing ratio, Glob. Chang. Biol., 18, 385–399, https://doi.org/10.1111/j.1365-2486.2011.02536.x, 2012.

Davis, P. A., Brown, J. C., Saunders, M., Lanigan, G., Wright, E., Fortune, T., Burke, J., Connolly, J., Jones, M. B., and Osborne, B.: Assessing the effects of agricultural management practices on carbon fluxes: Spatial variation and the need for replicated estimates of Net Ecosystem Exchange, Agric. For. Meteorol., 150, 564–574, https://doi.org/10.1016/j.agrformet.2010.01.021, 2010.

De Stefano, A. and Jacobson, M. G.: Soil carbon sequestration in agroforestry systems: a meta-analysis, Agrofor. Syst., 92, 285–299, https://doi.org/10.1007/s10457-017-0147-9, 2018.

Dias, N. L., Duarte, H. F., and Maggiotto, S. R.: An attenuated eddy covariance method for latent heat flux measurements, Water Resour. Res., 43, 1–9, https://doi.org/10.1029/2006WR005259, 2007.

Eugster, W. and Plüss, P.: A fault-tolerant eddy covariance system for measuring CH4fluxes, Agric. For. Meteorol., 150, 841–851, https://doi.org/10.1016/j.agrformet.2009.12.008, 2010.

Farahani, H. J., Howell, T. A., Shuttleworth, W. J., and Bausch, W. C.: Evapotranspiration: Progress in Measurement and Modeling in Agriculture, Am. Soc. Agric. Biol. Eng., 50, 1627–1638, 2007.

Foken, T.: Micrometorology, vol. 1, Springer-Verlag Berlin Heidelberg, Bayreuth, https://doi.org/10.1017/CBO9781107415324.004, 2008.

Foken, T. and Wichura, B.: Tools for quality assessment of surface-based flux measurements, Agric. For. Meteorol., 78, 83–105, 1996.

Foken, T., Göckede, M., Mauder, M., Mahrt, L., Amiro, B., and Munger, W.: Post-field data quality control, Handb. Micrometeorology, 29, 181–208, https://doi.org/10.1007/1-4020-2265-4_9, 2004.

Fratini, G., Ibrom, A., Arriga, N., Burba, G., and Papale, D.: Relative humidity effects on water vapour fluxes measured with closed-path eddy-covariance systems with short sampling lines, Agric. For. Meteorol., 165, 53–63, https://doi.org/10.1016/j.agrformet.2012.05.018, 2012.

Hill, T., Chocholek, M., and Clement, R.: The case for increasing the statistical power of eddy covariance ecosystem studies: why, where and how?, Glob. Chang. Biol., 23, 2154–2165, https://doi.org/10.1111/gcb.13547, 2017.

Ibrom, A., Dellwik, E., Flyvbjerg, H., Jensen, N. O., and Pilegaard, K.: Strong low-pass filtering effects on water vapour flux measurements with closed-path eddy correlation systems, Agric. For. Meteorol., 147, 140–156, https://doi.org/10.1016/j.agrformet.2007.07.007, 2007.

Kaimal, J. and Finnigan, J.: Atmospheric boundary layer flows: Their structure and measurement., Oxford University Press, New York, 1994.

Kaimal, J. C., Wyngaard, J. C., Izumi, Y., and Coté, O. R.: Spectral characteristics of surface layer turbulence, Q. J. R. Meteorol. Soc., 98, 563–589, https://doi.org/10.1002/qj.49709841707, 1972.

Katul, G. G., Oren, R., Manzoni, S., Higgins, C., and Parlange, M. B.: Evapotranspiration: a process driving mass transport and energy exchnge in the soil-plant-atmosphere-climate system, Rev. Geophys., 50, RG000 366: 1—-25, https://doi.org/10.1029/2011RG000366.1.INTRODUCTION, 2012.

Kljun, N., Calanca, P., Rotach, M. W., and Schmid, H. P.: A simple two-dimensional parameterisation for Flux Footprint Prediction (FFP), Geosci. Model Dev., 8, 3695–3713, https://doi.org/10.5194/gmd-8-3695-2015, 2015.

Kolmogorov, A. N.: The local structure of turbulence in incompressible viscous fluid for very large Reynolds numbers, Proc. R. Soc. London A Math. Phys. Eng. Sci., 434, 9–13, https://doi.org/10.1098/rspa.1991.0075, 1991.

Kristensen, L. and Fritzjarrals, D. R.: The Effect of Line Averaging on Scalar Flux Measurements with a Sonic Anemomete near the Surface, J. Atmos. Ocean. Technol., 1, 138–146, 1984.

Legendre, P. and Oksanen, J.: lmodel2: Model II Regression, Tech. rep., https://cran.r-project.org/web/packages/lmodel2/lmodel2.pdf, 2018.

Lenschow, D. H. and Raupach, M. R.: The attenuation of fluctuations in scalar concentrations through sampling tubes, J. Geophys. Res., 96, 15 259, https://doi.org/10.1029/91JD01437, 1991.

Leuning, R. and Moncrieff, J.: Eddy-covariance CO2 flux measurements using open- and closed-path CO2 analysers: Corrections for analyser water vapour sensitivity and damping of fluctuations in air sampling tubes, Boundary-Layer Meteorol., 53, 63–76, https://doi.org/10.1007/BF00122463, 1990.

LI-COR, I.: EddyPro 6 - Eddy Covariance Software Instruction Manual, Tech. rep., 2015.

Loescher, H. W., Law, B. E., Mahrt, L., Hollinger, D. Y., Campbell, J., Wofsy, S. C., Gu, L., Massman, W. J., Leuning, R., Pallardy, S. G., Meyers, T., Hanson, P. J., Riggs, J. S., Hosman, K. P., Yang, B., Hollinger, D. Y., Richardson, A. D., Goulden, M. L., Munger, J., Fan, S.-m., Daube, B. C., Wofsy, S. C., Louah, L., Visser, M., Blaimont, A., de Cannière, C., Oren, R., Hsieh, C. I., Stoy, P., Albertson, J., McCarthy, H. R., Harrell, P., Katul, G. G., Ong, C., Black, C., Wilson, J., Muthuri, C., Bayala, J., Jackson, N., Martel, M., Glenn, A., Wilson, H., Kröbel, R., Billesbach, D. P., Pérez-Priego, O., López-Ballesteros, A., Sánchez-Cañete, E. P., Serrano-Ortiz, P., Kutzbach, L., Domingo, F., Eugster, W., Kowalski, A. S., Haslwanter, A., Hammerle, A., Wohlfahrt, G., Baldocchi, D. D., Mauder, M., Zeeman, M. J., Gunawardena, N., Pardyjak, E., Stoll, R., Khadka, A., Wang, H., Tetzlaff, D., Soulsby, C., Chamberlain, S. D., Verfaillie, J., Eichelmann, E., Hemes, K. S., Baldocchi, D. D., Castellví, F., Oliphant, A., Wilczak, J. M., Oncley, S. P., and Stage, S. A.: Testing the maximum entropy production approach for estimating evapotranspiration from closed canopy shrubland in a low-energy humid environment, Agric. For. Meteorol., 25, 105–118, https://doi.org/10.1007/s10546-017-0275-9, http://dx.doi.org/10.1016/j.agrformet.2017.01.003http://dx.doi.org/10.1016/j.agrformet.2010.12.001https://doi.org/10.1016/j.ejrh.2017.11.010http://linkinghub.elsevier.com/retrieve/pii/B9780444525123000280http://dx.doi.org/10.1016/j.landusepol.2017.05., 2017.

Mann, J. and Lenschow, D. H.: Errors in airborne flux measurements, J. Geophys. Res., 99, 14 519, https://doi.org/10.1029/94JD00737, 1994.

Mauder, M. and Foken, T.: Impact of post-field data processing on eddy covariance flux estimates and energy balance closure, Meteorol. Zeitschrift, 15, 597–609, https://doi.org/10.1127/0941-2948/2006/0167, 2006.

Mauder, M. and Foken, T.: Documentation and Instruction Manual of the Eddy-Covariance Software Package TK3, Arbeitsergebnisse, pp. 60, ISSN 1614–8916, https://doi.org/10.5281/zenodo.20349, http://nbn-resolving.de/urn/resolver.pl?urn:nbn:de:bvb:703-opus-8665{%}5Cnhttp://opus4.kobv.de/opus4-ubbayreuth/frontdoor/index/index/docId/681, 2011a.

Mauder, M. and Foken, T.: Documentation and Instruction Manual of the Eddy-Covariance Software Package TK3, Univ. Bayreuth, Abt. Mikrometeorologie, pp. 1–60, 2011b.

Moncrieff, J., Massheder, J., de Bruin, H., Elbers, J., Friborg, T., Heusinkveld, B., Kabat, P., Scott, S., Soegaard, H., and Verhoef, A.: A system to measure surface fluxes of momentum, sensible heat, water vapour and carbon dioxide, J. Hydrol., 188-189, 589–611, https://doi.org/10.1016/S0022-1694(96)03194-0, 1997.

Moncrieff, J., Clement, R., Finnigan, J., and Meyers, T.: Averaging, Detrending, and Filtering of Eddy Covariance Time Series, Handb. Micrometeorology, 29, 7–31, https://doi.org/10.1007/1-4020-2265-4_2, 2004.

Polonik, P., Chan, W., Billesbach, D., Burba, G., Li, J., Nottrott, A., Bogoev, I., Conrad, B., and Biraud, S.: Comparison of gas analyzers for eddy covariance: Effects of analyzer type and spectral corrections on fluxes, Agric. For. Meteorol., 272-273, 128–142, https://doi.org/10.1016/j.agrformet.2019.02.010, https://linkinghub.elsevier.com/retrieve/pii/S0168192319300619, 2019.

Richardson, A. D., Hollinger, D. Y., Burba, G. G., Davis, K. J., Flanagan, L. B., Katul, G. G., William Munger, J., Ricciuto, D. M., Stoy, P. C., Suyker, A. E., Verma, S. B., and Wofsy, S. C.: A multi-site analysis of random error in tower-based measurements of carbon and energy fluxes, Agric. For. Meteorol., 136, 1–18, https://doi.org/10.1016/j.agrformet.2006.01.007, 2006.

Schmid, H. P.: Footprint modeling for vegetation atmosphere exchange studies: A review and perspective, Agric. For. Meteorol., 113, 159–183, https://doi.org/10.1016/S0168-1923(02)00107-7, 2002.

Schotanus, P., Nieuwstadt, F. T. M., and De Bruin, H. A. R.: Temperature measurement with a sonic anemometer and its application to heat and moisture fluxes, Boundary-Layer Meteorol., 26, 81–93, https://doi.org/10.1007/BF00164332, 1983.

Stull, R. B.: An introduction to boundary layer meteorology, https://doi.org/10.1007/978-94-009-3027-8, 1989.

Tang, X., Li, H., Desai, A. R., Nagy, Z., Luo, J., Kolb, T. E., Olioso, A., Xu, X., Yao, L., Kutsch, W., Pilegaard, K., Köstner, B., and Ammann, C.: How is water-use efficiency of terrestrial ecosystems distributed and changing on Earth?, Sci. Rep., 4, 7483, https://doi.org/10.1038/srep07483, 2014.

Trapletti, A. and Hornik, K.: tseries: Time Series Analysis and Computational Finance, Tech. rep., https://cran.r-project.org/package=tseries, 2017.

Vickers, D. and Mahrt, L.: Quality control and flux sampling problems for tower and aircraft data, J. Atmos. Ocean. Technol., 14, 512–526, https://doi.org/10.1175/1520-0426(1997)014<0512:QCAFSP>2.0.CO;2, 1997.

Webb, E. K., Pearman, G. I., and Leuning, R.: Correction of flux measurements for density effects due to heat and water vapour transfer, Q. J. R. Meteorol. Soc., 106, 85–100, https://doi.org/10.1002/QJ.49710644707, 1980.